Mathematics and Computers in Simulation 249 (2026) 1076–1113

Contents lists available at ScienceDirect

Mathematics and Computers in Simulation

journal homepage: www.elsevier.com/locate/matcom

Original articles

Mathematical analysis of HPV and gonorrhea co-infection model with optimal control strategies for effective intervention

M. Arunkumar [a,b], Sayooj Aby Jose [c,d,*], K. Murugesan [a], Anuwat Jirawattanapanit [e]

[a] Department of Mathematics, National Institute of Technology Tiruchirappalli, Tiruchirappalli, 620015, Tamil Nadu, India
[b] School of Artificial Intelligence, Sai University, Chennai, 603104, Tamil Nadu, India
[c] Institute for Data Innovation in Science, Seoul National University, Seoul, 08826, Republic of Korea
[d] Department of Statistics, Seoul National University, Seoul, 08826, Republic of Korea
[e] Department of Mathematics, Faculty of Education, Phuket Rajabhat University, Phuket, 83000, Thailand

ARTICLE INFO

Keywords:
HPV
Gonorrhea
Co-infection model
Data fitting
Optimal control
HPV vaccination

ABSTRACT

Human papillomavirus (HPV) and gonorrhea are sexually transmitted infections that pose significant challenges to global public health. This study introduces a novel mathematical model with eleven compartments to capture the dynamics between HPV and gonorrhea co-infection. We explore the basic analytical properties such as nonnegativity and boundedness of the solutions, stability analysis of disease-equilibrium point, existence of endemic equilibrium points for the co-infection model. The basic reproduction number is derived using next generation matrix method. Also, the model is calibrated and validated using real-world gonorrhea infection data from 2012 to 2022, collected in the United States to ensure its accuracy and relevance to current epidemiological trends. Sensitivity analysis is carried out to identify key parameters that influence the basic reproduction number. The findings reveal that reducing contact rates, increasing gonorrhea treatment rates, enhancing HPV vaccine efficacy, and accelerating HPV vaccination efforts substantially lower the disease transmission. Additionally, the effective contact rates of HPV and gonorrhea have been projected until 2062, providing valuable insights into the significance of reducing these infections. To further curb the transmission of these infections, three time-dependent control variables such as promoting safe sex practices, implementing a time-varying HPV vaccination rate and enhancing gonorrhea treatment are incorporated into the model. We then define an optimal control problem to minimize the total number of infected individuals and examine the existence of optimal control along with the necessary conditions for the optimality system. Numerical simulations are carried out to illustrate the practical implications of the model and the effectiveness of the proposed control strategies. The obtained results suggest that the simultaneous implementation of all control measures can significantly lower both single and co-infection rates, leading to improved public health outcomes.

* Corresponding author.
E-mail addresses: arunkumarmak001@gmail.com (M. Arunkumar), sayooj@snu.ac.kr (S.A. Jose), murugu@nitt.edu (K. Murugesan), anuwat.j@pkru.ac.th (A. Jirawattanapanit).

https://doi.org/10.1016/j.matcom.2026.06.027
Received 25 October 2024; Received in revised form 18 June 2026; Accepted 21 June 2026

Available online 26 June 2026
0378-4754/© 2026 International Association for Mathematics and Computers in Simulation (IMACS). Published by Elsevier B.V. All rights are reserved, including those for text and data mining, AI training, and similar technologies.

1. Introduction

Infectious diseases are caused by pathogenic microorganisms and can spread to susceptible hosts through contact with infected individuals, animals, or contaminated surfaces. These diseases can impact various parts of the body and may result in severe life-threatening conditions. The World Health Organization (WHO) reports that over 30 different bacteria, viruses and parasites can be transmitted through sexual contact, leading to various sexually transmitted infections (STIs). Additionally, STIs can be passed from a mother to her child during pregnancy, childbirth and breastfeeding. Eight pathogens are commonly associated with the highest rates of STIs. Four of these namely syphilis, chlamydia, trichomoniasis and gonorrhea are currently treatable. The other four include viral infections like hepatitis B, herpes simplex virus (HSV), human immunodeficiency virus (HIV) and human papillomavirus (HPV) are incurable [1].

Human papillomavirus (HPV) is the name of a group of 200 known viruses and is one of the most common STIs. The majority of sexually active individuals will encounter HPV during their lifetime, often without knowing the status as it typically remains asymptomatic. HPV can infect various parts of the body, including the skin, genital areas, and throat. Although condoms can reduce the risk of HPV transmission, they do not provide complete protection because they do not cover all of the genital skin [2]. According to the Centers for Disease Control and Prevention (CDC), three HPV vaccines namely the 9-valent HPV vaccine (Gardasil 9, 9vHPV), quadrivalent HPV vaccine (Gardasil, 4vHPV), and bivalent HPV vaccine (Cervarix, 2vHPV) have been licensed by the United States (U.S.) Food and Drug Administration [3]. All three HPV vaccines protect against HPV types 16 and 18 which cause most HPV cancers. Further, HPV commonly resolves on its own within two years in about 90% of cases. However, when it persists, it can lead to cancers of the cervix, vagina, vulva, penis, anus and throat, with approximately 36,000 cases of cancer occurring each year in the U.S. [4].

Gonorrhea is another STI caused by the bacterium *Neisseria gonorrhoeae* (*NG*) which specifically targets mucous membranes. In women, it affects the reproductive organs, including the cervix, uterus, and fallopian tubes, while in both men and women, it can infect the urethra. Additionally, the bacterium can also invade mucous membranes in the mouth, throat, eyes, and rectum [5]. Many women with gonorrhea may remain asymptomatic. However, when symptoms do appear, they may include a painful or burning sensation during urination, vaginal discharge and bleeding between periods or during sexual activity. In some cases, the infection can spread to the uterus or fallopian tubes, leading to pelvic inflammatory disease, which poses a risk of damaging the fallopian tubes, potentially causing infertility or increasing the risk of ectopic pregnancy. In men, typical symptoms include a burning sensation during urination and a white, yellow, or greenish discharge from the penis. Men may also experience complications such as epididymitis which is rare but can lead to infertility. If left untreated, gonorrhea can result in severe and long-lasting health complications in both genders. The infection is particularly prevalent in certain populations, including homosexual men, sex workers, and transgender women [6]. The CDC recommends treating gonorrhea with a single 500 mg intramuscular dose of ceftriaxone, which is considered effective. However, the growing issue of antimicrobial resistance in *NG* complicates treatment and makes eradicating the infection increasingly difficult [5]. This concern is underscored by WHO data showing that 82.4 million people aged 15 to 49 were newly infected with gonorrhea worldwide in 2020 [6].

Mathematical modeling is crucial for understanding infectious disease transmission and serves as a powerful tool for designing effective control measures [7–9]. In recent years, numerous mathematical models have been constructed to explore key epidemiological and clinical aspects of HPV infection, highlighting the importance of vaccination in disease management [10–13]. For instance, Saldaña et al. [14] developed a deterministic model to evaluate the impact of HPV immunization programs. They concluded that the most effective strategy is to allocate vaccines early in the epidemic and then gradually reduce vaccination rates as high coverage is achieved. In this direction, Gao et al. [15] formulated a deterministic model to study the transmission of HPV infection and the impact of vaccination in a heterosexually active population. Their analytical results demonstrated that a variable vaccination strategy, where more vaccines are administered initially is more effective in reducing HPV prevalence than evenly distributing vaccines over time.

In 1973, Cooke and Yorke [16] pioneered mathematical models to examine gonorrhea infection, focusing on a single homogeneous population and incorporating time delays to represent variations in the infectious period. Building on this foundation, Lajmanovich and Yorke [17] expanded the scope to nonhomogeneous populations, subdividing them into n homogeneous groups without time delays. Their model provided insights into the spread of gonorrhea across diverse groups. Following these initial studies, Mushayabasa and Bhunu [18] developed an epidemic model to investigate how heavy alcohol consumption affects gonorrhea transmission. Their numerical analysis revealed that higher rates of alcohol consumption correlate with increased transmission of the infection. Gkana and Zachilas [19] utilized a discrete-time deterministic model to study gonorrhea spread, emphasizing the importance of condom use in reducing transmission risk. Additionally, Adamu and Usman [20] contributed by developing a model that included factors like natural immunity and treatment. Their findings suggested that enhancing the treatment rate could significantly contribute to the eradication of gonorrhea.

Co-infection refers to the simultaneous presence of multiple infectious agents within a single individual. Recently, the Herbert Irving Comprehensive Cancer Center in the U.S. highlights that individuals infected with STIs such as chlamydia, gonorrhea, syphilis, or herpes are at an elevated risk of contracting HPV [21]. Supporting this, a study conducted by Lu et al. [22] at an outpatient clinic in Haikou, China, revealed that HPV-positive patients had markedly higher rates of co-infection with pathogens like *Chlamydia trachomatis* (*CT*), *Ureaplasma urealyticum* and *NG* compared to those who were HPV-negative. Additionally, nationwide data from Brazil revealed that 9.6% of sexually active young adults aged 16–25 had co-infections involving HPV and other STIs, with gonorrhea being the most frequently reported among HPV-positive individuals [23]. Further evidence from Bukowska et al. [24], based at the Medical University of Warsaw showed a high prevalence of HPV16 among women with chlamydia (58.3%) and gonorrhea (57.9%).

Their findings emphasized a significant link between HPV16 and these co-infections, suggesting that chlamydia and gonorrhea may play a role in the persistence of oncogenic HPV infections and elevate the risk of developing pre-cancerous lesions. Collectively, these results highlight the increasing prevalence of STIs and underscore the urgent need for comprehensive public health strategies to effectively manage and prevent co-infections, particularly those involving HPV and gonorrhea.

Over the past few decades, significant studies have been developed on modeling co-infections to uncover the factors that drive disease transmission and to gain a deeper understanding of infectious disease dynamics. Optimal control theory remains a powerful mathematical framework that serves as a key component in shaping decision-making processes in biological modeling [25,26]. It has found widespread application in exploring the dynamics of co-infections in epidemiology [27,28]. For example, Chukukere et al. [29] utilized a sex-structured model to evaluate the impact of treatment strategies targeting both chlamydia and gonorrhea in males and females through the application of optimal control. Additionally, Omame et al. [30] investigated the co-infection dynamics of HPV and CT, and identified via optimal control that the combined application of prevention strategies for both infections as the most cost-effective strategy. In parallel, Omame et al. [31] formulated a model to capture the combined effects of HPV vaccination and syphilis treatment on controlling HPV and syphilis co-infection. Their optimal control analysis provided valuable insights into reducing the burden of co-infection between the two diseases. Furthermore, numerous models focusing on co-infection diseases have been explored in the literature [32–37].

From the literature review, it is clear that both HPV and gonorrhea pose significant global public health implications. Understanding the interaction between these two diseases is crucial for developing effective prevention and treatment strategies. Despite evidence from medical research suggesting that HPV and gonorrhea can mutually influence and fuel each other, the comprehensive mathematical modeling of their co-infection dynamics remains unexplored. This study aims to address the gap by formulating a mathematical model to understand and control the co-infection of HPV and gonorrhea, particularly in the context of HPV vaccination and gonorrhea treatment interventions. To ensure the model accurately reflects real-world conditions, we calibrate and validate it with gonorrhea infection data from the U.S. collected over the period 2012 to 2022. Additionally, we incorporate three time-dependent control variables such as promoting safe sex practices, implementing time-varying HPV vaccination rate and enhancing gonorrhea treatment. The ultimate aim is to provide policymakers with the insights necessary to develop effective control measures that align with real-world situations.

The significant contributions of this article are systematically presented as follows: Section 2 introduces the co-infection model, encompassing eleven compartments that represent various interactions of HPV and gonorrhea infections. The fundamental properties focusing on nonnegativity, boundedness, derivation of the basic reproduction number and the stability of the disease-free equilibrium point, existence of endemic equilibrium points are established in Section 3. The model is then fitted to real-world data, with relevant parameters estimated using gonorrhea infection data from the U.S., as detailed in Section 4. Section 5 is dedicated to conduct a sensitivity analysis to identify the key parameters that influence the behavior of the model. Numerical results and discussions presented in Sections 6 and 7 offer practical insights into the biological implications of the co-infection model. Section 8 defines the optimal control problem, examines the existence of optimal control and necessary conditions for optimality system, and further provides numerical illustrations to highlight its significance. Finally, Section 9 concludes the article by summarizing the main findings. The analysis of HPV and gonorrhea submodels are detailed in Appendix.

2. Mathematical model formulation

In this section, a novel deterministic mathematical model is formulated to study the interactions between HPV and gonorrhea. The model comprises of eleven compartments representing different states of individuals concerning HPV and gonorrhea infections, along with HPV vaccination and gonorrhea treatment. This model partitions the total sexually active population at time t, denoted as $N(t)$, into the following compartments: susceptible individuals ($S(t)$), HPV vaccinated individuals ($V_H(t)$), asymptomatic HPV infected individuals ($A_H(t)$), symptomatic HPV infected individuals ($I_H(t)$), HPV recovered individuals ($R_H(t)$), asymptomatic gonorrhea infected individuals ($A_G(t)$), symptomatic gonorrhea infected individuals ($I_G(t)$), co-infected individuals with HPV and gonorrhea ($I_{HG}(t)$), gonorrhea infected individuals receiving treatment ($T_G(t)$), co-infected individuals receiving gonorrhea treatment ($T^G_{HG}(t)$), gonorrhea recovered individuals ($R_G(t)$). Therefore, $N = S + V_H + A_H + I_H + R_H + A_G + I_G + I_{HG} + T_G + T^G_{HG} + R_G$.

New sexually active individuals are recruited into the susceptible population at the rate of $(1-\gamma)\Lambda$, where γ represents the proportion of individuals who have been vaccinated against HPV before reaching age 15, as routine HPV vaccination is typically recommended for those who aged between 11 and 12 years. HPV vaccination is generally not advised for individuals over 26 years old. However, people aged between 27 and 45 who were not vaccinated earlier can opt it after consulting with their healthcare provider. Consequently, these individuals may enter the vaccination compartment at a rate of ϑ. The efficacy and waning rate of the vaccine are represented by the parameters ϵ and θ respectively. Additionally, the risk of contracting HPV and gonorrhea among individuals is governed by the respective effective transmission rates, denoted as λ_H and λ_G. The force of HPV infection is given by $\lambda_H = \dfrac{\beta_H(A_H + \psi_1 I_H + \psi_2 I_{HG} + \psi_3 T^G_{HG})}{N}$, where β_H is the effective contact rate for HPV transmission. The parameters ψ_1 and ψ_2 are assumed to be greater than 1 that represent the increased infectiousness of individuals infected with HPV and those who are co-infected with gonorrhea. These parameters reflect heightened transmissibility and susceptibility among individuals in these states. In contrast, ψ_3 is constrained to the range of 0 to 1, indicating less pronounced effects on transmission.

The force of gonorrhea infection is described by $\lambda_G = \dfrac{\beta_G(A_G + \phi_1 I_G + \phi_2 T_G + \phi_3 I_{HG} + \phi_4 T^G_{HG})}{N}$, where β_G denotes the effective contact rate for gonorrhea transmission. The parameters ϕ_1, ϕ_2 (or ϕ_4) and ϕ_3 capture the relative infectiousness associated with individuals infected with gonorrhea, those receiving gonorrhea treatment and those co-infected with both gonorrhea and HPV

respectively. Notably, ϕ_1 and ϕ_3 are greater than 1, indicating increased transmissibility among these groups, while ϕ_2 and ϕ_4 is within the range of 0 to 1, reflecting a less pronounced effect.

Asymptomatic HPV infected individuals can progress to symptomatic HPV infected at a rate of σ or recover naturally at a rate of ϵ_1. Symptomatic HPV infected individuals may move to the HPV recovered compartment through natural recovery at a rate of ϵ_2. Asymptomatic gonorrhea infected individuals become symptomatic gonorrhea infected at a rate of σ_1. Symptomatic gonorrhea individuals receive treatment at a rate of ω. Subsequently, individuals receiving gonorrhea treatment recover and transition to the gonorrhea recovered compartment at a rate of γ_1.

The modification parameters α_1, α_2, α_3, and α_4 capture the enhanced infectiousness and susceptibility associated with co-infection between HPV and gonorrhea. Specifically, α_1 and α_2 reflect increased transmission of gonorrhea from asymptomatic and symptomatic HPV, respectively, while α_3 and α_4 represent heightened susceptibility to HPV among individuals with asymptomatic and symptomatic gonorrhea, respectively. Each α_i is greater than 1, indicating a significant interplay between the two infections. Further, individuals co-infected with HPV and gonorrhea are treated for gonorrhea alone at a rate denoted by ω_1, transitioning to the treatment compartment (T^G_{HG}). After the treatment, they may move to HPV only infected at the rate of η. Moreover, the parameter κ_1 indicate the loss of immunity to HPV and κ_2 reflects the loss of immunity to gonorrhea after recovery. The mortality rates due to HPV infection are captured by δ_1 and δ_2 for asymptomatic and symptomatic cases, respectively. Additionally, δ_3 represents the additional mortality rate for individuals co-infected with both HPV and gonorrhea, whereas δ_4 accounts for the mortality rate of co-infected individuals specifically under gonorrhea treatment. It is assumed that μ represents a common natural death rate for all compartments. Further, it is assumed that all the parameters are nonnegative. For better presentation, Fig. 1 illustrates the dynamics of HPV and gonorrhea co-infection, highlighting the interactions between infection, vaccination, progression, treatment and recovery.

Based on the above assumptions, the deterministic co-infection model is formulated as the following nonlinear system of ordinary differential equations:

$$\begin{aligned}
\frac{dS}{dt} &= (1-\gamma)\Lambda - \lambda_H S - \lambda_G S + \theta V_H - (\vartheta+\mu)S + \kappa_1 R_H + \kappa_2 R_G,\\
\frac{dV_H}{dt} &= \gamma\Lambda + \vartheta S - (1-\epsilon)\lambda_H V_H - \lambda_G V_H - (\theta+\mu)V_H,\\
\frac{dA_H}{dt} &= \lambda_H S + (1-\epsilon)\lambda_H V_H - \alpha_1\lambda_G A_H - (\sigma+\epsilon_1+\mu+\delta_1)A_H,\\
\frac{dI_H}{dt} &= \sigma A_H - \alpha_2\lambda_G I_H + \eta T^G_{HG} - (\epsilon_2+\mu+\delta_2)I_H,\\
\frac{dR_H}{dt} &= \epsilon_1 A_H + \epsilon_2 I_H - (\kappa_1+\mu)R_H,\\
\frac{dA_G}{dt} &= \lambda_G V_H + \lambda_G S - \alpha_3\lambda_H A_G - (\sigma_1+\mu)A_G,\\
\frac{dI_G}{dt} &= \sigma_1 A_G - \alpha_4\lambda_H I_G - (\omega+\mu)I_G,\\
\frac{dI_{HG}}{dt} &= (\alpha_1 A_H + \alpha_2 I_H)\lambda_G + (\alpha_3 A_G + \alpha_4 I_G)\lambda_H - (\omega_1+\mu+\delta_3)I_{HG},\\
\frac{dT_G}{dt} &= \omega I_G - (\gamma_1+\mu)T_G,\\
\frac{dT^G_{HG}}{dt} &= \omega_1 I_{HG} - (\eta+\mu+\delta_4)T^G_{HG},\\
\frac{dR_G}{dt} &= \gamma_1 T_G - (\kappa_2+\mu)R_G,
\end{aligned} \tag{1}$$

with nonnegative initial conditions

$$\left.\begin{aligned}
&S(0)>0, V_H(0)\geq 0, A_H(0)>0, I_H(0)>0, R_H(0)\geq 0,\\
&A_G(0)>0, I_G(0)>0, I_{HG}(0)>0, T_G(0)\geq 0, T^G_{HG}(0)\geq 0, R_G(0)\geq 0.
\end{aligned}\right\} \tag{2}$$

3. Analytical studies of the co-infection model

To facilitate the qualitative analysis of the co-infection model (1), we analyze the gonorrhea and HPV submodels in Appendices A and B, respectively. The analysis of nonnegativity and boundedness is fundamental in epidemiological modeling, as they help to ensure that the population of individuals remains nonnegative and does not grow infinitely over time. This section explores these two properties in the context of the co-infection model (1). Let us consider, $\mathbb{R}^n_+ = \{(x_1, x_2, \dots, x_n) \in \mathbb{R}^n : x_i \geq 0, i = 1, 2, \dots, n\}$.

3.1. Biological well-posedness of the model (1)

Theorem 3.1. *Any solution of the system (1), that is*

$$(S(t), V_H(t), A_H(t), I_H(t), R_H(t), A_G(t), I_G(t), I_{HG}(t), T_G(t), T^G_{HG}(t), R_G(t))$$

with initial conditions as in (2) remains nonnegative for all time $t \geq 0$.

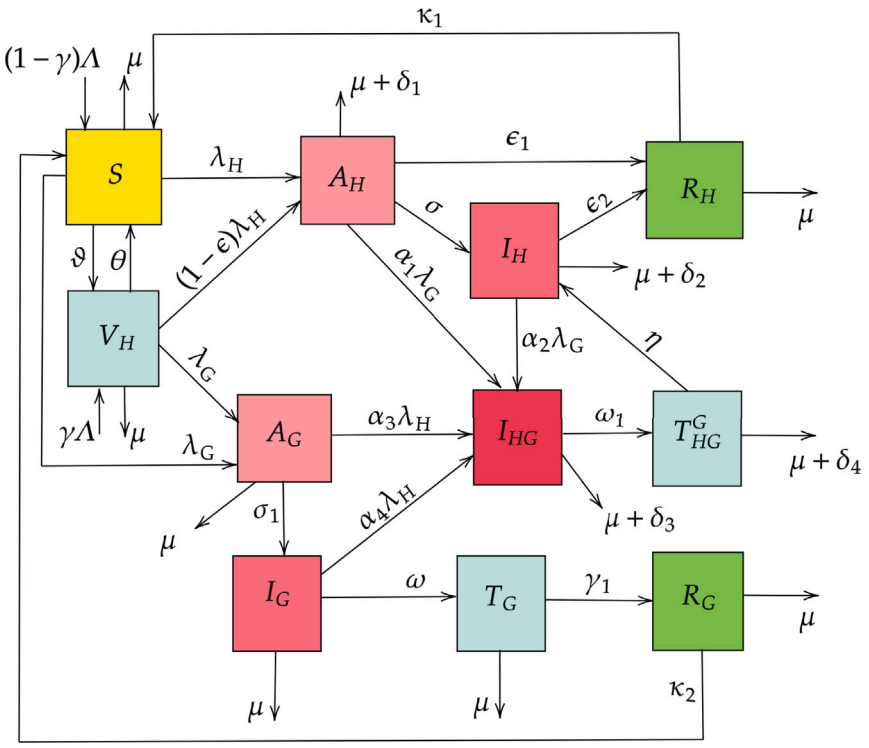

Fig. 1. Schematic flow diagram of HPV and gonorrhea co-infection model.

Proof. The proof is based on the same arguments as in the proof of Theorem A.1. □

Theorem 3.2. *The solution of the system (1) is bounded in the biologically feasible region given by*

$$\Xi_3 = \left\{ (S, V_H, A_H, I_H, R_H, A_G, I_G, I_{HG}, T_G, T^G_{HG}, R_G) \in \mathbb{R}^{11}_+ : 0 \le N \le \frac{\Lambda}{\mu} \right\}.$$

Further, Ξ_3 is a positively invariant and attracting set.

Proof. By employing arguments as in Theorem B.2, it can be shown that Ξ_3 is bounded, positively invariant and attracting set [38]. □

Theorem 3.3. *For any nonnegative initial conditions, the system (1)–(2) admits a unique global solution in $\mathbb{R}^{11}_+$.*

Proof. Each function on the right-hand side of (1) is continuous and locally Lipschitz on the region $\mathbb{R}^{11}_+$. Hence, by the Picard–Lindelöf theorem, a unique solution of the system (1)–(2) exists on a time interval $[0, b)$ with $b \in [0, \infty)$. Theorem 3.2 shows that the solution of the system (1) remains bounded in the region Ξ_3. Thus, from Corollary A.5 given in [39], the system (1)–(2) admits a unique global solution. □

3.2. Existence of DFE and basic reproduction number

In this subsection, we prove that the disease-free equilibrium (DFE) point of the system (1) exists and derive the basic reproduction number $\mathcal{R}_0$ for the co-infection model (1). First, the DFE point E° of the system (1) is determined by equating its right-hand side to zero and assuming the infected compartments to be zero. Thus,

$$E^\circ = (S^\circ, V_H^\circ, 0, 0, 0, 0, 0, 0, 0, 0, 0) = \left(\frac{\Lambda(\theta + (1-\gamma)\mu)}{\mu(\theta + \vartheta + \mu)}, \frac{\Lambda(\vartheta + \gamma\mu)}{\mu(\theta + \vartheta + \mu)}, 0, 0, 0, 0, 0, 0, 0, 0, 0 \right).$$

The basic reproduction number $\mathcal{R}_0$ is a key epidemiological metric that quantifies the potential for disease spread in a population. It represents the average number of secondary infections produced by a single infected individual in a completely susceptible population [40]. The derivation of $\mathcal{R}_0$ for the model (1) is carried out by employing the next generation matrix method [41]. With the aid of Appendices A.2 and B.2, it is found that $\mathcal{R}_0 = \max\{\mathcal{R}_{0H}, \mathcal{R}_{0G}\}$. Here,

$$\mathcal{R}_{0H} = \frac{\beta_H(\theta + (1-\epsilon)\vartheta + (1-\gamma\epsilon)\mu)(\mu + \delta_2 + \epsilon_2 + \sigma\psi_1)}{(\theta + \mu + \vartheta)(\mu + \sigma + \epsilon_1 + \delta_1)(\mu + \delta_2 + \epsilon_2)}, \tag{3}$$

and

$$\mathcal{R}_{0G} = \frac{\beta_G((\omega+\mu)(\gamma_1+\mu)+\phi_1\sigma_1(\gamma_1+\mu)+\phi_2\sigma_1\omega)}{(\mu+\sigma_1)(\mu+\omega)(\gamma_1+\mu)}. \tag{4}$$

It emphasizes that the prevalence and persistence of disease in the community are driven by the more dominant infection either HPV or gonorrhea.

3.3. Stability analysis of DFE point

Theorem 3.4. *The DFE point (E°) for the co-infection system (1) is locally asymptotically stable (LAS) if $\mathcal{R}_0 < 1$ and unstable if $\mathcal{R}_0 > 1$.*

Proof. The result follows directly from the approach utilized in [41]. For completeness, the detailed proof is provided in Appendix C. □

Theorem 3.5. *In the absence of co-infection ($\alpha_i = 0, i = 1,2,3,4$), the DFE point ($E^\circ$) for the co-infection system (1) is globally asymptotically stable (GAS) if $\mathcal{R}_0 < 1$.*

Proof. This theorem can be proved by using Lemma A.4. Now for the system (1), let $\mathcal{X} = (S, V_H, R_H, R_G) \in \mathbb{R}^4$ and $\mathcal{K} = (A_H, I_H, A_G, I_G, I_{HG}, T_G, T_{HG}^G) \in \mathbb{R}^7$. To prove the condition $(W1)$, consider the following subsystem:

$$\begin{aligned}
\frac{dS}{dt} &= (1-\gamma)\Lambda + \theta V_H - (\vartheta+\mu)S + \kappa_1 R_H + \kappa_2 R_G,\\
\frac{dV_H}{dt} &= \gamma\Lambda + \vartheta S - (\theta+\mu)V_H,\\
\frac{dR_H}{dt} &= -(\kappa_1+\mu)R_H,\\
\frac{dR_G}{dt} &= -(\kappa_2+\mu)R_G.
\end{aligned} \tag{5}$$

Following the ideas outlined in the proof of Theorem B.4, it follows that $(S^\circ, V_H^\circ, 0, 0)$ is GAS for the subsystem (5).

By computation, we estimate

$$\widehat{\mathcal{Q}}(\mathcal{X},\mathcal{K}) = \begin{bmatrix}
\beta_H(A_H+\psi_1 I_H+\psi_2 I_{HG}+\psi_3 T_{HG}^G)\left(\dfrac{S^\circ+(1-\epsilon)V_H^\circ}{S^\circ+V_H^\circ} - \dfrac{S+(1-\epsilon)V_H}{N}\right)\\
\alpha_2\lambda_G I_H\\
\alpha_3\lambda_H A_G + \beta_G(A_G+\phi_1 I_G+\phi_2 T_G+\phi_3 I_{HG}+\phi_4 T_{HG}^G)\left(1-\dfrac{S+V_H}{N}\right)\\
\alpha_4\lambda_H A_G\\
-(\alpha_1 A_H+\alpha_2 I_H)\lambda_G - (\alpha_3 A_G+\alpha_4 I_G)\lambda_H\\
0\\
0
\end{bmatrix}.$$

From above, it is found that $\widehat{\mathcal{Q}}(\mathcal{X},\mathcal{K}) \geq \mathbf{0}$, whenever $\alpha_i = 0, i = 1,2,3,4$ and $(\mathcal{X},\mathcal{K}) \in \Xi_3$. Using Lemma A.4, the DFE point E° of the system (1) is found to be GAS if $\mathcal{R}_0 < 1$ and $\alpha_i = 0, i = 1,2,3,4$. □

3.4. Existence of endemic equilibria

In this subsection, we derive two disease-persistent boundary endemic equilibrium points of system (1), namely: (i) the gonorrhea-only endemic equilibrium, and (ii) the HPV-only endemic equilibrium.

(i) The gonorrhea-only endemic equilibrium is given by $E_{0G}^* = (S^*, 0, 0, 0, 0, A_G^*, I_G^*, 0, T_G^*, 0, R_G^*)$, where

$$S^* = \frac{\Lambda}{\mu+\lambda_G^*\left(1-\dfrac{\kappa_2\gamma_1\omega\sigma_1}{(\kappa_2+\mu)(\gamma_1+\mu)(\omega+\mu)(\sigma_1+\mu)}\right)}, A_G^* = \frac{\lambda_G^* S^*}{\sigma_1+\mu}, I_G^* = \frac{\sigma_1 A_G^*}{\omega+\mu}, T_G^* = \frac{\omega\sigma_1 A_G^*}{(\gamma_1+\mu)(\omega+\mu)},$$

and $R_G^* = \dfrac{\gamma_1\omega\sigma_1 A_G^*}{(\kappa_2+\mu)(\gamma_1+\mu)(\omega+\mu)}$.

Substituting all the steady-state expressions into λ_G^* yields

$$\lambda_G^* = \frac{(\sigma_1+\mu)(\mathcal{R}_{0G}-1)}{\left(1+\dfrac{\sigma_1}{\omega+\mu}+\dfrac{\omega\sigma_1}{(\gamma_1+\mu)(\omega+\mu)}+\dfrac{\gamma_1\omega\sigma_1}{(\kappa_2+\mu)(\gamma_1+\mu)(\omega+\mu)}\right)}.$$

Hence, if $\mathcal{R}_{0G} > 1$, then the gonorrhea-only endemic equilibrium exists and is unique.

(ii) The HPV-only endemic equilibrium is given by $E^*_{H0} = (S^*, V^*_H, A^*_H, I^*_H, R^*_H, 0, 0, 0, 0, 0, 0)$, where

$$S^* = \frac{A_1\lambda^*_H + A_0}{B_2(\lambda^*_H)^2 + B_1\lambda^*_H + B_0}, V^*_H = \frac{\gamma\Lambda + \vartheta S^*}{(1-\epsilon)\lambda^*_H + (\theta+\mu)}, A^*_H = \frac{\lambda^*_H\left(S^* + (1-\epsilon)V^*_H\right)}{C_2},$$
$$I^*_H = \frac{\sigma A^*_H}{\epsilon_2+\mu+\delta_2}, \text{ and } R^*_H = \frac{(\epsilon_1(\epsilon_2+\mu+\delta_2)+\epsilon_2\sigma)A^*_H}{(\kappa_1+\mu)(\epsilon_2+\mu+\delta_2)}.$$

Substituting the steady-state equilibrium expressions into λ^*_H gives,

$$P_3\lambda^{*3}_H + P_2\lambda^{*2}_H + P_1\lambda^*_H + P_0 = 0, \tag{6}$$

After algebraic simplification, we obtain $P_3 < 0$ and $P_0 = \Lambda C_2^2\mu D_0(\vartheta+\mu+\theta)(\mathcal{R}_{0H}-1)$. The expressions for constants are given in Appendix D. Thus, the existence of E^*_{H0} depends on the existence of positive real roots of the cubic Eq. (6).

(a) **Case I:** $\mathcal{R}_{0H} > 1$**.** In this case, $P_0 > 0$ and $P_3 < 0$. Thus, the sign of the coefficients of Eq. (6) is $(P_3, P_2, P_1, P_0) = (-, \pm, \pm, +)$. By Descartes' rule of signs, depending on the signs of P_2 and P_1, the system may admit exactly one positive real root, or three positive real roots. Therefore, the model can exhibit a unique endemic equilibrium or multiple endemic equilibria.

(b) **Case II:** $\mathcal{R}_{0H} < 1$**.** In this case, $P_0 < 0$ and $P_3 < 0$. By Descartes' rule of signs, the cubic Eq. (6) admits either no positive real root, or two positive real roots. Hence, even when $\mathcal{R}_{0H} < 1$, the possibility of two positive endemic equilibria indicates the chance of occurrence of backward bifurcation.

(c) **Case III:** $\mathcal{R}_{0H} = 1$**.** In this case, $P_0 = 0$, and Eq. (6) reduces to $\lambda^*_H\left(P_3\lambda^{*2}_H + P_2\lambda^*_H + P_1\right) = 0$. Thus, one trivial root is $\lambda^*_H = 0$, corresponding to the disease-free equilibrium. The remaining quadratic equation determines the existence of non-trivial endemic equilibria. Depending on the discriminant $(P_2^2 - 4P_3P_1)$, the system may admit either no endemic equilibrium or one/two positive endemic equilibria.

(iii) Obtaining explicit analytical expressions for the endemic equilibrium with the presence co-infection case is highly challenging due to the nonlinear coupling of the system. However, numerical simulations of the infected class I_{HG} for $\mathcal{R}_0 > 1$ suggests the existence of an interior endemic equilibrium (see, Fig. 7).

4. Model calibration

In this section, we calibrate the model parameters using real-world data specific to the United States (U.S.). As per the 2012 census, the total U.S. population was estimated to be 308,827,000 [42]. Within this population, the total sexually active individuals (aged 15 – 64 years) in 2012 was determined to be 206,189,000. The World Data Bank reports the life expectancy in the U.S. as 78.74 years [43]. Consequently, the natural death rate is calculated as $\mu = \frac{1}{78.74} = 0.0127$, and the recruitment rate is given by $\Lambda = \mu N = 2618600$. According to CDC report, 334,826 individuals were infected with gonorrhea in 2012 [44]. For this study, we set the baseline year as 2012 ($t = 0$).

According to the National Cancer Institute, approximately 80 million people in the U.S. were infected with HPV in 2012 [45]. The CDC reports that 70% to 90% of these cases remain asymptomatic. Based on this information, the initial conditions (in million) are taken as follows: $S(0) = 108.791$, $V_H(0) = 3.091$, $A_H(0) = 56$, $I_H(0) = 24$, $R_H(0) = 10$, $A_G(0) = 0.4$, $I_G(0) = 0.334826$, $I_{HG}(0) = 3.392$, $T_G(0) = 0.1$, $T^G_{HG}(0) = 0.03$, $R_G(0) = 0.05$.

The CDC reports that the majority of individuals infected with HPV do not develop symptoms or experience health problems, and in the most cases (9 out of 10), HPV resolves on its own within two years [4]. Accordingly, the natural recovery rate ϵ_1 is assumed to be 0.5. Furthermore, clinical trial results indicate that HPV vaccines are highly effective in preventing infections, leading to the assumption of HPV vaccine efficacy ϵ as 0.95 [46]. Consequently, the rate at which vaccinated individuals return to the susceptible class, θ is assumed to be 0.05. Based on a cancer trends report from 2012 [47], 17.21% of adolescents aged 13 – 15 years had received 2 or 3 doses of HPV vaccine, which we use to estimate the proportion of vaccinated individuals, γ as 0.1721. Additional parameters related to HPV have been carefully selected from existing literature and are summarized in Table 1.

The yearly reported data on gonorrhea cases from 2012 to 2022 were taken from the CDC [48]. By employing *lsqcurvefit* from MATLAB R2023b with parameter and initial values held fixed as previously described, the other parameters of the model is obtained and given in Table 1. The fitting of yearly reported gonorrhea cases to the solution of $I_G(t)$ from system (1) is shown in Fig. 2. The residuals plot indicates a reasonable fit for the model, and the Mean Absolute Percentage Error (MAPE) was found to be 2.3757%. All parameters used in the model are described and their corresponding values are provided in Table 1.

4.1. Dynamics of the model without control variables

From the parameter values given in Table 1, the basic reproduction number for gonorrhea and HPV are evaluated to be $\mathcal{R}_{0G} = 0.68730$ and $\mathcal{R}_{0H} = 0.17123$, respectively. Thus, the basic reproduction number for the co-infection system is determined as $\mathcal{R}_0 = \max\{0.68730, 0.17123\} = 0.68730 < 1$. Given that $\mathcal{R}_0 < 1$, the disease is expected to eventually die out within the population under the current conditions. Fig. 3 illustrates the solutions of the model (1), showing a decline in the number of infected individuals over time, ultimately leading to the elimination of the disease. This outcome underscores the effectiveness of the chosen parameters in controlling the spread of both HPV and gonorrhea.

Table 1
Parameter descriptions and values.

Parameters	Description	Values	Sources
Λ	Human recruitment rate	2 618 600	Estimated
β_G	Effective contact rate for gonorrhea transmission	0.17226	Fitted
β_H	Effective contact rate for HPV transmission	0.78588	Fitted
γ	A proportion of people receiving HPV vaccination	0.1721	[47]
μ	Natural death rate for humans	0.0127	Estimated
ϵ	Efficacy of HPV vaccine	0.95	[46]
θ	HPV vaccine waning rate	0.05	Assumed
ϑ	Rate of susceptible individuals getting HPV vaccination	0.623	Fitted
σ	Rate of progression from asymptomatic HPV infected to symptomatic	0.5	[49]
σ_1	Rate of progression from asymptomatic gonorrhea infected to symptomatic	0.7123	Fitted
ϵ_1	Natural recovery rate of asymptomatic HPV infected	0.5	[50]
ϵ_2	Natural recovery rate of symptomatic HPV infected	0.9	[51]
κ_1	Loss of immunity to HPV	0.1	Assumed
κ_2	Loss of immunity to gonorrhea	0.22592	Fitted
ω, ω_1	Gonorrhea treatment rate	0.45521, 0.15224	Fitted
γ_1	Gonorrhea recovery rate	0.74570	Fitted
η	Gonorrhea recovery rate of co-infected individuals	0.34544	Fitted
δ_1, δ_2	HPV induced mortality rate	0.001, 0.01	[49,52]
δ_3, δ_4	HPV induced mortality rate among co-infected	0.05, 0.03	Assumed
$\phi_1, \phi_2, \phi_3, \phi_4$	Modification parameters to measure the relative infectiousness	1.02890, 0.35720,1.31051,0.31230	Fitted
$\alpha_1, \alpha_2, \alpha_3, \alpha_4$	Modification parameters to measure the relative infectiousness	1.24804,1.36690,1.35120,1.45860	Fitted
ψ_1, ψ_2, ψ_3	Modification parameters to measure the relative infectiousness	1.2,1.3,0.4	Assumed

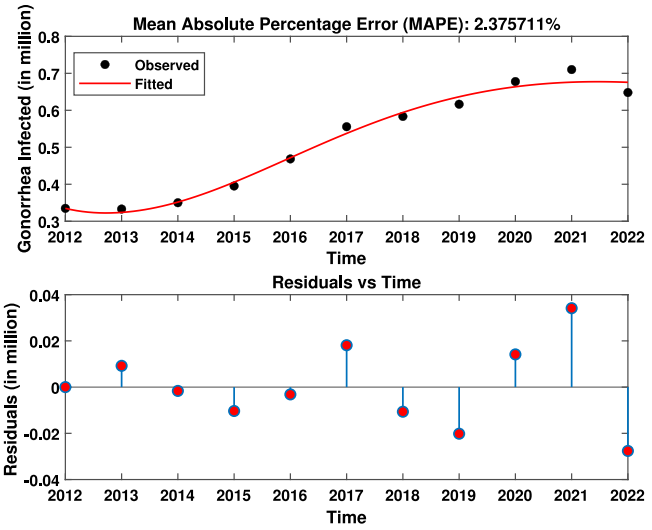

Fig. 2. Fitting of yearly reported gonorrhea cases with model predictions.

To study the long-term dynamics and to illustrate the disease-free, boundary endemic, and interior endemic equilibria, of the system (1), numerical simulations are performed using five distinct sets of initial conditions (ICs) (in millions), representing a broad range of initial infection levels:

1. IC1: $S(0) = 108.791$, $V_H(0) = 3$, $A_H(0) = 56$, $I_H(0) = 24$, $R_H(0) = 10$, $A_G(0) = 0.4$, $I_G(0) = 0.334826$, $I_{HG}(0) = 3.392$, $T_G(0) = 0.1$, $T_{HG}(0) = 0.03$, $R_G(0) = 0.05$.
2. IC2: $S(0) = 175.719$, $V_H(0) = 5$, $A_H(0) = 20$, $I_H(0) = 3$, $R_H(0) = 5$, $A_G(0) = 0.2$, $I_G(0) = 0.1$, $I_{HG}(0) = 1$, $T_G(0) = 0.03$, $T_{HG}(0) = 0.01$, $R_G(0) = 0.07$.
3. IC3: $S(0) = 96.979$, $V_H(0) = 7$, $A_H(0) = 60$, $I_H(0) = 30$, $R_H(0) = 8$, $A_G(0) = 0.5$, $I_G(0) = 0.5$, $I_{HG}(0) = 3$, $T_G(0) = 0.05$, $T_{HG}(0) = 0.06$, $R_G(0) = 0.09$.
4. IC4: $S(0) = 60.789$, $V_H(0) = 10$, $A_H(0) = 66$, $I_H(0) = 47$, $R_H(0) = 15$, $A_G(0) = 1$, $I_G(0) = 1$, $I_{HG}(0) = 8$, $T_G(0) = 0.2$, $T_{HG}(0) = 0.1$, $R_G(0) = 0.1$.
5. IC5: $S(0) = 41.139$, $V_H(0) = 4$, $A_H(0) = 80$, $I_H(0) = 69$, $R_H(0) = 20$, $A_G(0) = 2$, $I_G(0) = 1.5$, $I_{HG}(0) = 10$, $T_G(0) = 0.3$, $T_{HG}(0) = 0.15$, $R_G(0) = 0.1$.

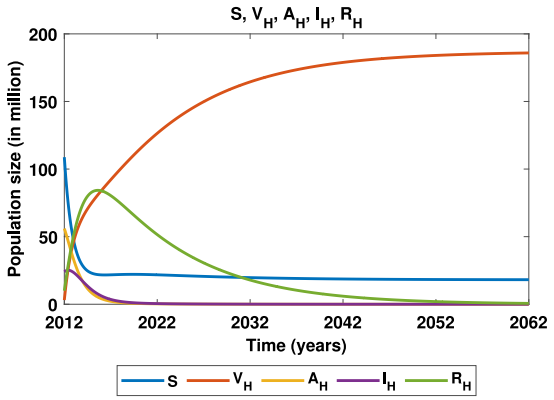

(a) Susceptible and HPV-only compartments

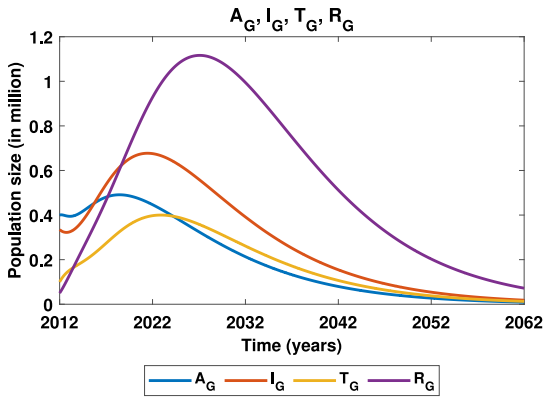

(b) Gonorrhea-only compartments

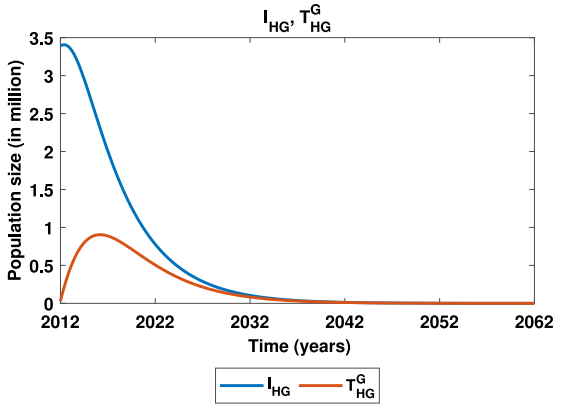

(c) Co-infected compartments

Fig. 3. Solutions of the co-infection model (1).

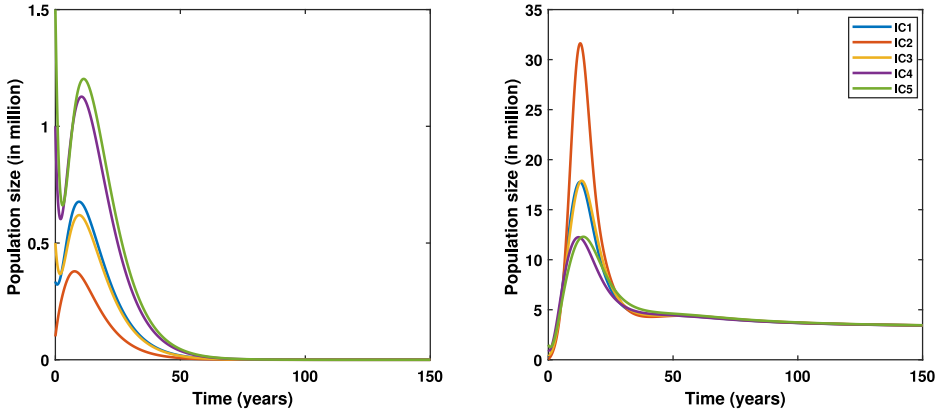

Fig. 4. Dynamics of I_G when $\mathcal{R}_{0G} < 1$ (left panel) and $\mathcal{R}_{0G} > 1$ (right panel).

For $\beta_G = 0.67226$ and the remaining parameter values given in Table 1, we obtain $\mathcal{R}_{0G} = 2.68225 > 1$. The existence analysis therefore predicts a unique gonorrhea-only endemic equilibrium E^*_{0G}. As shown in Fig. 4 (right panel), the trajectories of the gonorrhea-infected compartment I_G approach a positive steady-state value for all initial conditions, indicating persistence of gonorrhea infection. In contrast, when $\mathcal{R}_{0G} = 0.6873 < 1$, the trajectories converge to zero, corresponding to disease elimination (see Fig. 4 left panel). These observations agree with the theoretical result that the gonorrhea-only endemic equilibrium exists only when $\mathcal{R}_{0G} > 1$.

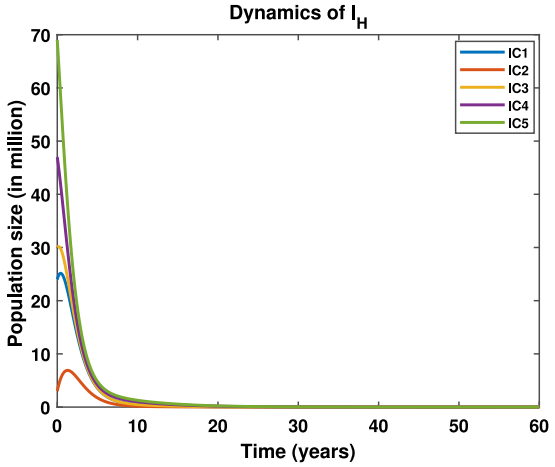

Fig. 5. Dynamics of I_H when $R_{0H} < 1$.

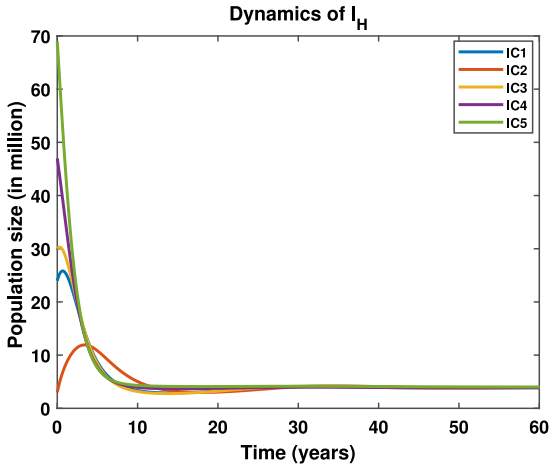

Fig. 6. Dynamics of I_H when $R_{0H} > 1$.

For the baseline parameter values listed in Table 1, we have $\mathcal{R}_{0H} < 1$, and Eq. (6) admits no positive root. Consequently, no HPV-only endemic equilibrium exists. This behavior is confirmed in Fig. 5, where the trajectories of I_H decay to zero for all initial conditions, indicating convergence to the disease-free state. To illustrate the HPV-only endemic equilibrium, we consider $\beta_H = 0.98588$, $\gamma = 0.01$, $\vartheta = 0.06$, $\theta = 0.01$, and $\epsilon = 0.05$, while keeping the remaining parameters as in Table 1. For this parameter set, we obtain $\mathcal{R}_{0H} = 1.54663 > 1$. Moreover, the cubic Eq. (6) satisfies $P_1 > 0$ and $P_2 < 0$, yielding a unique positive root and hence the HPV-only endemic equilibrium E^*_{H0}. Fig. 6 shows that the trajectories of I_H converge to the same positive steady state for all five initial conditions, supporting the existence of the HPV-only endemic equilibrium. Although the theoretical analysis permits the existence of multiple HPV endemic equilibria and backward bifurcation under certain parameter regimes, such scenarios are not observed for the parameter values estimated from the U.S. epidemiological data considered in this study. However, the investigation of multiple endemic equilibria and backward bifurcation under alternative parameter settings is left for future research.

Further, for the parameters values $\beta_G = 0.67226$, $\beta_H = 0.98588$, $\gamma = 0.01, \vartheta = 0.06$, $\theta = 0.01$, $\epsilon = 0.05$ along with other parameter values as in Table 1, we get $\mathcal{R}_{0G} = 2.68225$ and $\mathcal{R}_{0H} = 1.54663$, respectively. Then, the basic reproduction number for the co-infection system is determined as $\mathcal{R}_0 = \max\{2.68225, 1.54663\} = 2.68225 > 1$. Fig. 7 depicts the trajectories of the co-infected compartment I_{HG} for the five initial conditions. It is observed that all trajectories converge to the same positive steady-state value, indicating persistence of the co-infection. This numerical behavior provides evidence for the existence of an interior endemic equilibrium of the full co-infection model.

In practice, control strategies are often constrained by various practical factors such as limited public health resources, budget restrictions, high costs of sustained interventions, and the societal and economic burdens associated with persistent infection. To address these challenges, we introduce an optimal control framework that incorporates time-dependent intervention variables such

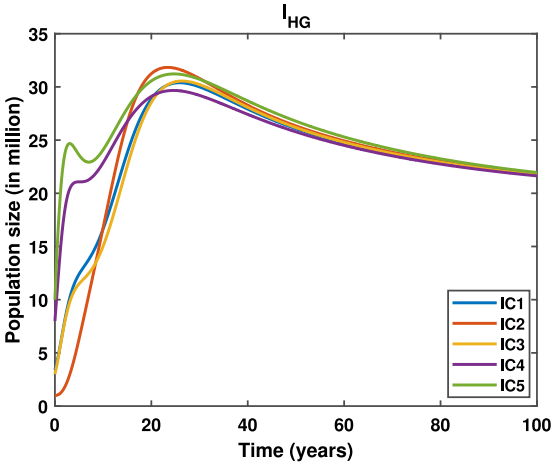

Fig. 7. Dynamics of I_{HG} when $R_0 > 1$.

Table 2
Normalized forward sensitivity indices of $\mathcal{R}_{0G}$ and $\mathcal{R}_{0H}$ associated with model parameters.

Normalized sensitivity index	Value	Normalized sensitivity index	Value
$\Upsilon^{\mathcal{R}_{0G}}_{\beta_G}$	1.000	$\Upsilon^{\mathcal{R}_{0H}}_{\beta_H}$	1.0000
$\Upsilon^{\mathcal{R}_{0G}}_{\phi_1}$	0.5415	$\Upsilon^{\mathcal{R}_{0H}}_{\theta}$	0.4719
$\Upsilon^{\mathcal{R}_{0G}}_{\phi_2}$	0.1128	$\Upsilon^{\mathcal{R}_{0H}}_{\epsilon}$	−6.4717
$\Upsilon^{\mathcal{R}_{0G}}_{\omega}$	−0.5237	$\Upsilon^{\mathcal{R}_{0H}}_{\vartheta}$	−0.5691
$\Upsilon^{\mathcal{R}_{0G}}_{\gamma_1}$	−0.1109	$\Upsilon^{\mathcal{R}_{0H}}_{\gamma}$	−0.0226
$\Upsilon^{\mathcal{R}_{0G}}_{\sigma_1}$	−0.3282	$\Upsilon^{\mathcal{R}_{0H}}_{\delta_2}$	−0.0043
$\Upsilon^{\mathcal{R}_{0H}}_{\epsilon_2}$	−0.3843	$\Upsilon^{\mathcal{R}_{0H}}_{\sigma}$	−0.0992
$\Upsilon^{\mathcal{R}_{0H}}_{\psi_1}$	0.3940	$\Upsilon^{\mathcal{R}_{0H}}_{\epsilon_1}$	−0.4932
		$\Upsilon^{\mathcal{R}_{0H}}_{\delta_1}$	−0.00098

as prevention efforts, vaccination, and treatment into the disease dynamics. These controls facilitate the design of strategies that minimize both the infection burden and intervention costs over a finite time horizon. Accordingly, optimal control ensures that the implemented interventions are both effective and resource-efficient.

Before formulating the optimal control problem, we conduct a sensitivity analysis to better understand the influence of key parameters on the behavior of the model. This analysis identifies which parameters have the most significant impact on disease progression and intervention effectiveness. The insights gained are then used to fine-tune the timing and intensity of interventions within the optimal control model, ultimately maximizing the health outcomes while minimizing costs.

5. Sensitivity analysis

Sensitivity analysis is conducted to assess the relative influence of each parameter on the basic reproduction number. Following the method proposed by Chitnis et al. [53], the normalized forward sensitivity index on $\mathcal{S}$ with respect to the parameter ς is given by,

$$\Upsilon^{\mathcal{S}}_{\varsigma} = \frac{\varsigma}{\mathcal{S}} \frac{\partial \mathcal{S}}{\partial \varsigma}.$$

Utilizing the parameter values from Table 1, the normalized sensitivity indices for the basic reproduction number of gonorrhea ($\mathcal{R}_{0G}$) and HPV ($\mathcal{R}_{0H}$), associated with various model parameters are shown in Table 2 and can be visualized in Fig. 8.

A positive sensitivity index signifies that an increase in the parameter value leads to a proportional rise in the corresponding basic reproduction number, which directly amplifies disease transmission. For instance, the effective contact rates β_G and β_H are the most influential drivers of $\mathcal{R}_{0G}$ and $\mathcal{R}_{0H}$, respectively, with both exhibiting a normalized sensitivity index of 1.000. This unit sensitivity index indicates that a 1% increase in β_G and β_H results in a corresponding 1% increase in $\mathcal{R}_{0G}$ and $\mathcal{R}_{0H}$, respectively. In addition, the modification parameters ϕ_i (for $i = 1, 2$) and ψ_1, which represent the relative infectiousness of individuals with gonorrhea and HPV respectively, also exhibit positive sensitivity indices, highlighting their significant role in sustaining transmission. Since these parameters reflect the frequency and riskiness of sexual contact between susceptible and infectious individuals, any increase in

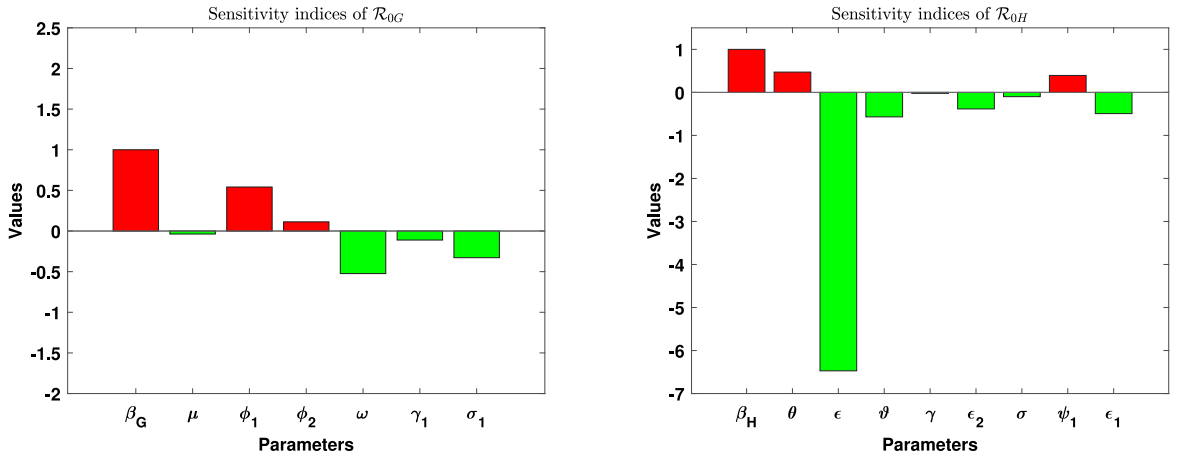

(a) Sensitivity indices of $\mathcal{R}_{0G}$

(b) Sensitivity indices of $\mathcal{R}_{0H}$

Fig. 8. Sensitivity indices for $\mathcal{R}_{0G}$ and $\mathcal{R}_{0H}$.

transmission rates can directly intensify the spread of both diseases. Moreover, the asymptomatic nature of these infections in many cases allows for silent transmission, complicating efforts to control their spread within the population. Therefore, targeting these parameters is crucial for controlling the spread of both diseases. Effective strategies such as sexual behavior modification through public health campaigns promoting condom use, reducing the number of sexual partners, and encouraging regular screenings for high-risk individuals can serve as a cornerstone of public health efforts to reduce the burden of gonorrhea and HPV. On the other hand, the HPV vaccine waning rate (θ) exhibits a positive sensitivity index of 0.4719, indicating that as immunity wanes faster, $\mathcal{R}_{0H}$ increases accordingly. This emphasizes the critical need for vaccines that remain potent and effective over long duration to ensure sustained HPV prevention.

Conversely, a negative sensitivity index means that as the parameter value increases, the reproduction number decreases, thereby reducing the overall disease burden. For example, the sensitivity indices $Y_{\omega}^{\mathcal{R}_{0G}} = -0.5237$ and $Y_{\epsilon}^{\mathcal{R}_{0H}} = -6.4717$ indicate that increases in the gonorrhea treatment rate (ω) and HPV vaccine efficacy (ϵ) lead to substantial reductions in $\mathcal{R}_{0G}$ and $\mathcal{R}_{0H}$, respectively. Specifically, a 1% increase in ϵ could yield a more than 6% reduction in $\mathcal{R}_{0H}$, making it the most impactful parameter for HPV control in this analysis. Similarly, increasing ω significantly reduces $\mathcal{R}_{0G}$, highlighting the importance of timely and effective treatment interventions in curbing gonorrhea spread. For gonorrhea, the intervention strategy should focus on strengthening health infrastructure to ensure earlier diagnosis and prompt treatment. For HPV, improving vaccine coverage and uptake, especially in populations with limited access and ensuring the use of highly efficacious vaccines can drastically reduce transmission. In addition, the vaccination rate for HPV (ϑ), also shows a notable negative sensitivity index (-0.5691), reinforcing the importance of broad immunization campaigns. These findings suggest that enhancing access to treatment services and improving vaccine performance are critical components of an effective public health response. Thus, the insights from sensitivity analysis elucidate key drivers of disease transmission and guide targeted interventions to maximize control efforts and improve public health outcomes.

6. Effects of sensitive parameters on $\mathcal{R}_0$

Building on the findings from the sensitivity analysis, this section examines the influence of key parameters on the basic reproduction number $\mathcal{R}_0$. As $\mathcal{R}_0 = \max\{\mathcal{R}_{0G}, \mathcal{R}_{0H}\}$, the impact of model parameters on $\mathcal{R}_{0G}$ and $\mathcal{R}_{0H}$ are studied separately in the forthcoming subsections.

6.1. Effects of model parameters on $\mathcal{R}_{0G}$

In this subsection, contour plots have been utilized to examine the relationship between $\mathcal{R}_{0G}$ and various parameters such as β_G, ϕ_1, ϕ_2, ω, γ_1 and σ_1.

(i) **Impact of β_G and ω on $\mathcal{R}_{0G}$:** Fig. 9(a) demonstrates that the effective contact rate for gonorrhea transmission (β_G) has a strong positive influence on the basic reproduction number $\mathcal{R}_{0G}$, indicating a higher potential for the disease to spread as β_G increases. In contrast, the gonorrhea treatment rate (ω) exerts a negative effect on $\mathcal{R}_{0G}$, highlighting the importance of effective treatment strategies in reducing transmission.
The relationship between $\mathcal{R}_{0G}$ and β_G is further explored in Fig. 9(b), which suggests that decreasing β_G can bring $\mathcal{R}_{0G}$ below 1, potentially slowing the spread of the disease. Fig. 9(c) emphasizes the significant impact of increasing ω in reducing $\mathcal{R}_{0G}$, thereby lowering the potential of the disease spread. Therefore, preventive strategies should aim to reduce β_G through public health campaigns promoting safe sexual practices, alongside widespread screening, early diagnosis and increasing ω by improving access to effective gonorrhea treatment to curb transmission (see Fig. 9).

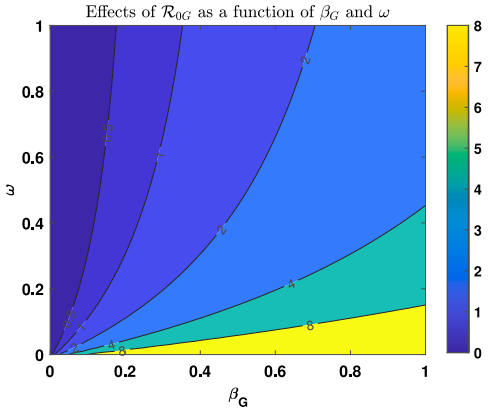

(a) Effects of β_G and ω on $\mathcal{R}_{0G}$

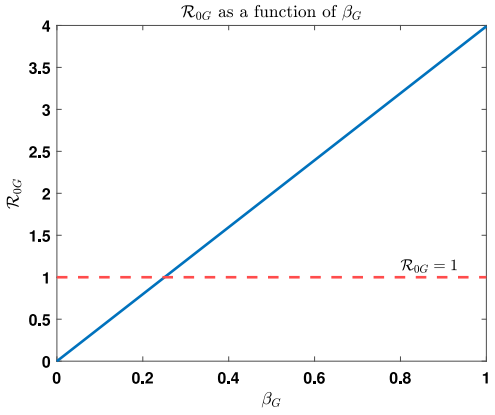

(b) Effects of β_G on $\mathcal{R}_{0G}$

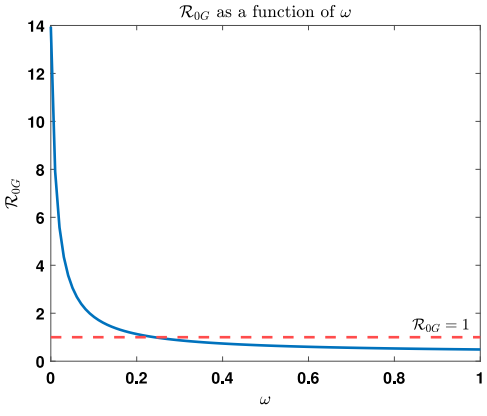

(c) Effects of ω on $\mathcal{R}_{0G}$

Fig. 9. Effects of β_G and ω on $\mathcal{R}_{0G}$.

(ii) **Role of ϕ_1, ϕ_2 and ω on $\mathcal{R}_{0G}$:** Fig. 10 illustrates that the modification parameters ϕ_1 and ϕ_2, which account for the relatively high infectiousness of symptomatic gonorrhea infected and co-infected individuals is found to contribute an increase in $\mathcal{R}_{0G}$ significantly. Conversely, an increase in ω is shown to reduce $\mathcal{R}_{0G}$, underscoring the critical role of effective treatment in curbing disease spread. To further control gonorrhea transmission, the implementation of targeted interventions, as discussed in (i), is essential. These measures including enhancing treatment accessibility, promoting early diagnosis and encouraging behavioral changes are vital in reducing the spread of the disease.

(iii) **Influence of σ_1 and γ_1 on $\mathcal{R}_{0G}$:** Fig. 11(a) shows that the increase in rate of progression from asymptomatic to symptomatic gonorrhea infection (σ_1) increases $\mathcal{R}_{0G}$. This suggests that faster progression leads to a higher reproduction number, making the infection more difficult to control. On the other hand, the gonorrhea recovery rate (γ_1) decreases $\mathcal{R}_{0G}$, emphasizing the importance of improving recovery rates to control the epidemic. This is further captured through Fig. 11(b). The control strategies should focus on early detection and treatment of asymptomatic cases to slow down the progression to symptomatic stages, thereby reducing $\mathcal{R}_{0G}$. Enhancing recovery rates through effective treatment strategies should also be prioritized to lower the overall transmission potential (see Fig. 11).

6.2. Effects of model parameters on $\mathcal{R}_{0H}$

This subsection analyzes the variations in key parameters that influence $\mathcal{R}_{0H}$ under a vaccination strategy, highlighting their impact on HPV transmission dynamics.

(i) **β_H vs $\mathcal{R}_{0H}$:** Fig. 12 illustrates the relationship between $\mathcal{R}_{0H}$ and the effective contact rate for HPV transmission β_H. As β_H increases, $\mathcal{R}_{0H}$ rises proportionally, demonstrating that higher transmission rates significantly amplify the spread of HPV. Despite this increase, $\mathcal{R}_{0H}$ reaches only 0.218 when β_H is set to 1, which is a direct consequence of the vaccination effects incorporated into the model. The subsequent points will further detail this observation.

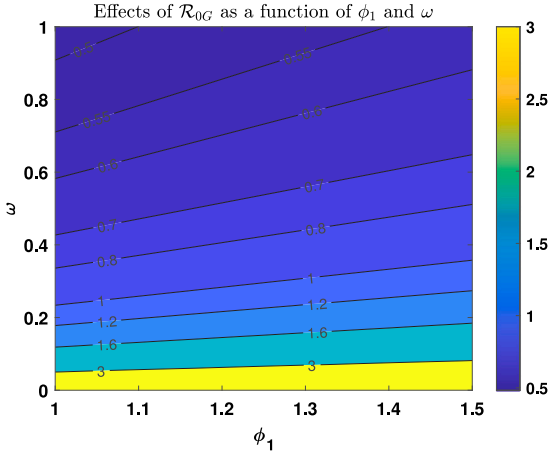

(a) Effects of ϕ_1 and ω on $\mathcal{R}_{0G}$

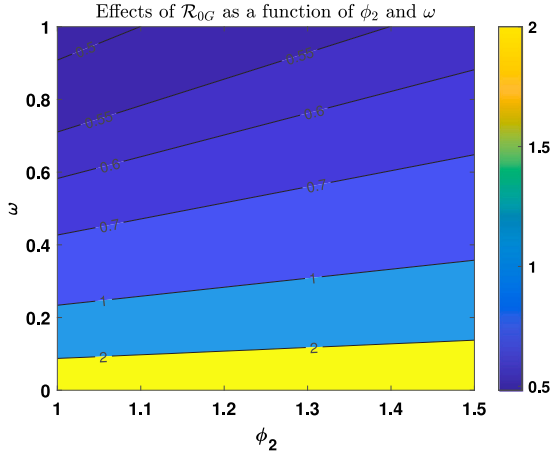

(b) Effects of ϕ_2 and ω on $\mathcal{R}_{0G}$

Fig. 10. Effects of ϕ_1, ϕ_2 and ω on $\mathcal{R}_{0G}$.

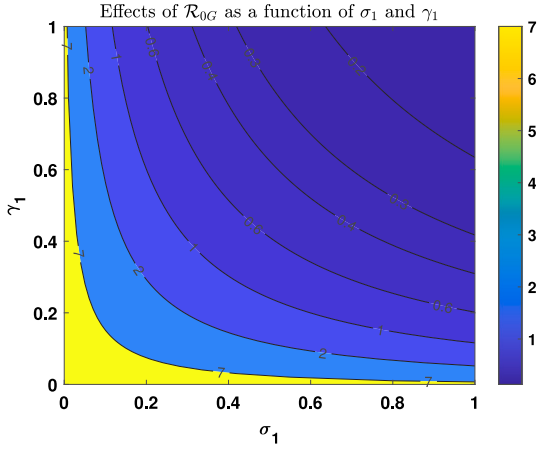

(a) Effects of σ_1 and γ_1 on $\mathcal{R}_{0G}$

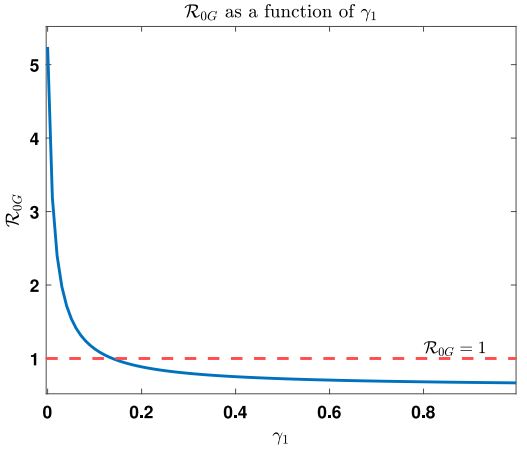

(b) Effects of γ_1 on $\mathcal{R}_{0G}$

Fig. 11. Effects of σ_1 and γ_1 on $\mathcal{R}_{0G}$.

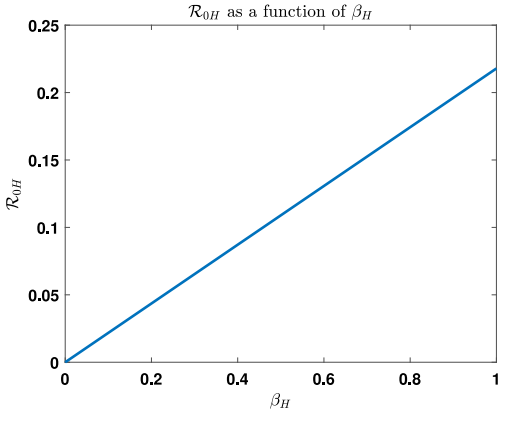

Fig. 12. Effect of β_H on $\mathcal{R}_{0H}$.

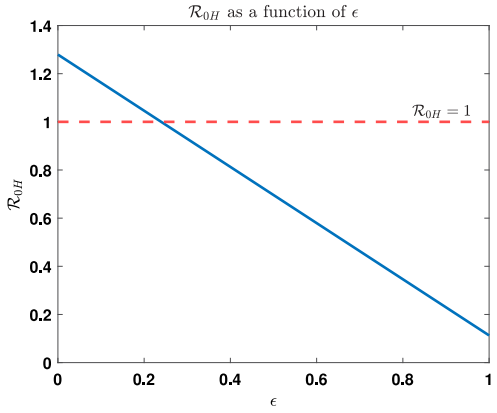

Fig. 13. Effect of ϵ on $\mathcal{R}_{0H}$.

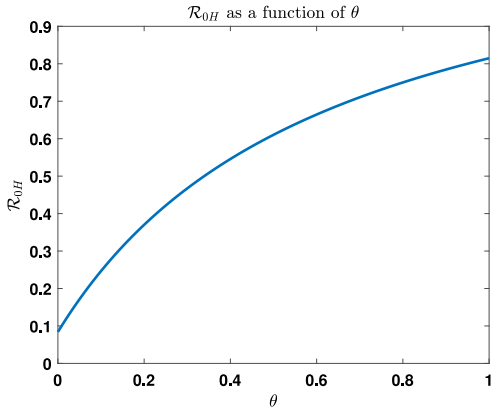

Fig. 14. Effect of θ on $\mathcal{R}_{0H}$.

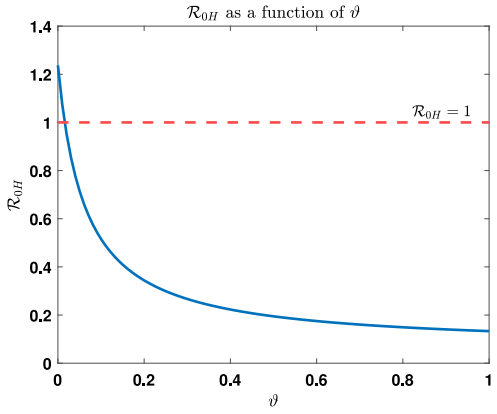

Fig. 15. Effect of ϑ on $\mathcal{R}_{0H}$.

(ii) ϵ **vs** $\mathcal{R}_{0H}$**:** Fig. 13 depicts the effect of vaccine efficacy ϵ on $\mathcal{R}_{0H}$. As vaccine efficacy increases, $\mathcal{R}_{0H}$ decreases. This underscores the importance of effective vaccines that play a crucial role in controlling HPV transmission. A highly efficacious vaccine significantly reduces the number of new infections by enhancing immunity within the vaccinated population, thereby lowering the overall infection risk. This reduction in $\mathcal{R}_{0H}$ is vital for ensuring that a sufficient proportion of the population is protected against HPV.

(iii) θ **vs** $\mathcal{R}_{0H}$**:** Fig. 14 examines the impact of the HPV vaccine waning rate θ on $\mathcal{R}_{0H}$. An increased waning rate results in a higher $\mathcal{R}_{0H}$, indicating that as the protective effect of the vaccine diminishes over time, the population becomes more susceptible to

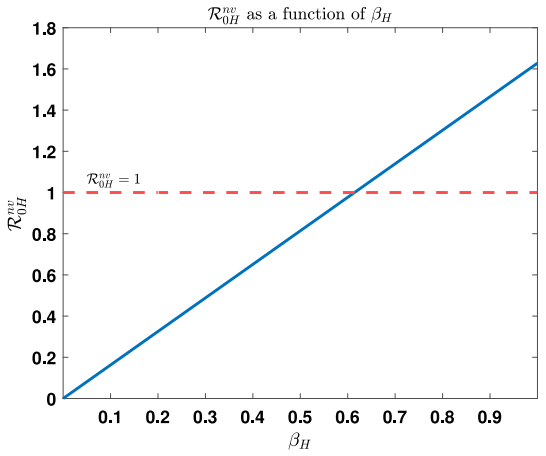

Fig. 16. Effect of β_H on $\mathcal{R}_{0H}^{nv}$.

HPV transmission. This highlights the importance of continuous monitoring of vaccine efficacy and potentially administering additional doses to sustain immunity and prevent an increase in $\mathcal{R}_{0H}$.

(iv) ϑ **vs** $\mathcal{R}_{0H}$**:** Fig. 15 examines the influence of the rate at which susceptible individuals receive HPV vaccination ϑ on $\mathcal{R}_{0H}$. The figure reveals that as ϑ increases, $\mathcal{R}_{0H}$ decreases, underscoring the significance of high vaccination coverage in reducing HPV transmission. Enhancing vaccination rates among susceptible is crucial for lowering $\mathcal{R}_{0H}$, thereby reducing the likelihood of disease transmission within the population. This emphasizes the need of widespread and accessible vaccination programs to achieve significant reductions in HPV prevalence.

Collectively, these findings highlight the pivotal role of vaccination in controlling HPV transmission. By reducing β_H, increasing ϵ, addressing θ and enhancing ϑ, it is possible to keep $\mathcal{R}_{0H}$ below the threshold required for sustained transmission. This not only curtails the spread of HPV but also contributes to long-term public health benefits, including the potential for HPV eradication in the future. Vaccination remains one of the most effective strategies in the fight against HPV, significantly aiding in the control and prevention of the HPV transmission among individuals.

6.3. Effects of model parameters on $\mathcal{R}_{0H}$ without vaccination

In this section, we investigate the effects of various model parameters on the basic reproduction number for HPV ($\mathcal{R}_{0H}$) in the absence of vaccination. Previous simulations demonstrated that the HPV vaccine, particularly when administered at the recommended age of 11–12 years, consistently resulted in $\mathcal{R}_{0H}$ values below 1. However, to thoroughly analyze the influence of different parameters on HPV transmission, we redefine the basic reproduction number by excluding the effects of vaccination ($\vartheta = \theta = \epsilon = \gamma = 0$), yielding a new measure, $\mathcal{R}_{0H}^{nv}$. The formula for $\mathcal{R}_{0H}^{nv}$ is simplified as:

$$\mathcal{R}_{0H}^{nv} = \frac{\beta_H(\mu + \delta_2 + \epsilon_2 + \sigma\psi_1)}{(\mu + \sigma + \epsilon_1 + \delta_1)(\mu + \delta_2 + \epsilon_2)}. \tag{7}$$

This reproduction number reflects the transmission potential of HPV based solely on natural infection dynamics, excluding any mitigating effects from vaccination.

Fig. 16 visualizes the impact of the effective contact rate for HPV transmission on $\mathcal{R}_{0H}^{nv}$. The plot demonstrates a clear direct relationship between β_H and $\mathcal{R}_{0H}^{nv}$, indicating that as the contact rate increases, the potential for HPV to spread within the population also rises. This underscores the critical need for interventions that reduce β_H, such as promoting safe sexual practices and increasing public awareness, especially in scenarios where vaccination is not feasible or where vaccination coverage remains low.

Further analysis of Fig. 17 reveals the significant influence of β_H and the modification parameter ψ_1 on $\mathcal{R}_{0H}^{nv}$. An increase in β_H directly raises $\mathcal{R}_{0H}^{nv}$, highlighting the importance of transmission rates in determining the overall reproduction number. Meanwhile, ψ_1 modifies the term $\sigma\psi_1$ in the numerator of (7), adjusting for the relative infectiousness of individuals already infected with HPV. A higher value of ψ_1 increases the potential for transmission, thereby elevating $\mathcal{R}_{0H}^{nv}$ and indicating a greater risk of HPV spread within the population.

The analysis of $\mathcal{R}_{0H}^{nv}$ without vaccination highlights the key role of β_H in HPV transmission and the impact of ψ_1. While vaccination is vital, the findings underscore the need for measures to reduce transmission and control HPV in non-vaccination scenarios.

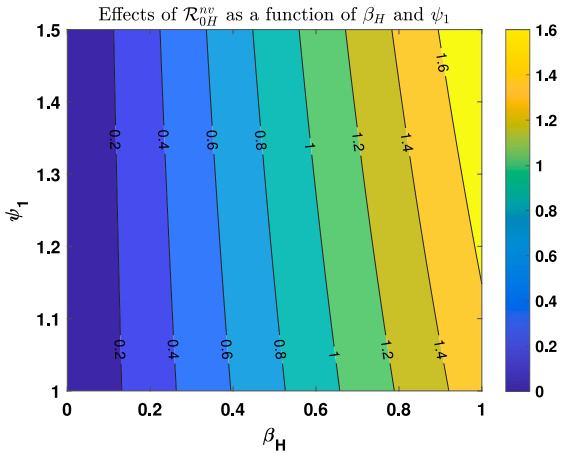

Fig. 17. Effect of β_H and ψ_1 on $\mathcal{R}_{0H}^{nv}$.

7. Influences of β_G and β_H in long-term model predictions

This section presents long-term projections of model (1), that calibrated with gonorrhea case data from 2012 to 2022, by varying key transmission parameters β_G and β_H. While we cannot change the past, these variations allow us to forecast the future and enhance the understanding of how these parameters influence the dynamics of HPV and gonorrhea co-infection. This study provides valuable insights for policymakers and enable them to make decisions to control both infections effectively.

7.1. Influence of β_G on infected compartments

(i) **Impacts of β_G on $A_G(t)$:** First, the significant changes in the number of asymptomatic gonorrhea infected individuals ($A_G(t)$) under various values of β_G is observed in Fig. 18. As β_G decreases, the peak number of asymptomatic infections diminishes. For instance, with $\beta_G = 0.97226$, the model predicts 36.4865 million infected individuals by 2030. As β_G is reduced to 0.87226, 0.77226, 0.67226, and 0.37226, the maximum number of infected individuals decreases to 33.237 million in 2031, 29.645 million in 2032, 25.7867 million in 2034, and 10.8929 million in 2061, respectively. Comparatively, the fitted value of $\beta_G = 0.17226$ results in a peak of 0.491045 million asymptomatic infected individuals in 2018, after which the infection begins to decline (see Fig. 3(b)).

(ii) **Impacts of β_G on $I_G(t)$:** The effect of varying β_G on the number of symptomatic gonorrhea infected individuals ($I_G(t)$) is also evident from Fig. 19, revealing how changes in the transmission rate impact the severity of the gonorrhea epidemic. With a higher transmission rate of $\beta_G = 0.97226$, the maximum number of symptomatic infections reached 45.1108 million individuals around 2031. As β_G decreases, the peak number of symptomatic individuals also decreases, with 42.3561 million individuals at $\beta_G = 0.87226$ in 2033, 39.0223 million individuals at $\beta_G = 0.77226$ in 2034, 35.1408 million individuals at $\beta_G = 0.67226$ in 2036, 16.4698 million individuals at $\beta_G = 0.37226$ in 2062. In contrast to these scenarios, the baseline fitted value of $\beta_G = 0.17226$ yields the lowest peak in symptomatic infections, reaching 0.67731 million individuals, after which the number continues to decline steadily (see Fig. 3(b)).
These results highlight that higher transmission rates lead to more severe and earlier peaks in asymptomatic and symptomatic gonorrhea infections, affecting a larger number of individuals. Conversely, lower transmission rates result in reduced infections and delayed peaks, indicating a slower and less intense disease spread.

(iii) **Impacts of β_G on $I_{HG}(t)$:** Additionally, we examine how the behavior of co-infected individuals changes with varying values of β_G. As observed from Fig. 20, increased values of β_G lead to a significant increase in the size of the co-infection compartment initially, followed by a decline towards the end of the prediction period. For instance, with $\beta_G = 0.97226$, the model predicts that 56.714 million people will be co-infected by 2048. At $\beta_G = 0.87226$, this number reduces to 54.0924 million by 2040. For β_G values of 0.77226 and 0.67226, the number of co-infected individuals reaches 59.867 million and 46.773 million by 2052 and 2056 respectively. Conversely, lower values of β_G such as 0.37226 and 0.17226 demonstrate a decreasing trend in the number of co-infected individuals. This indicates that decreasing the transmission rate of gonorrhea not only reduces the number of gonorrhea only infected individuals but also significantly lowers the incidence of HPV-infected individuals with gonorrhea.

This analysis indicates that reducing β_G emerges as a key factor in lowering gonorrhea infections. Strategies such as early diagnosis, prompt treatment, robust public health campaigns and widespread screening can significantly reduce both asymptomatic and symptomatic cases. Since asymptomatic infections contribute to unnoticed transmission, comprehensive approaches combining behavioral interventions with public health measures are essential. Additionally, screening for gonorrhea in HPV infected individuals

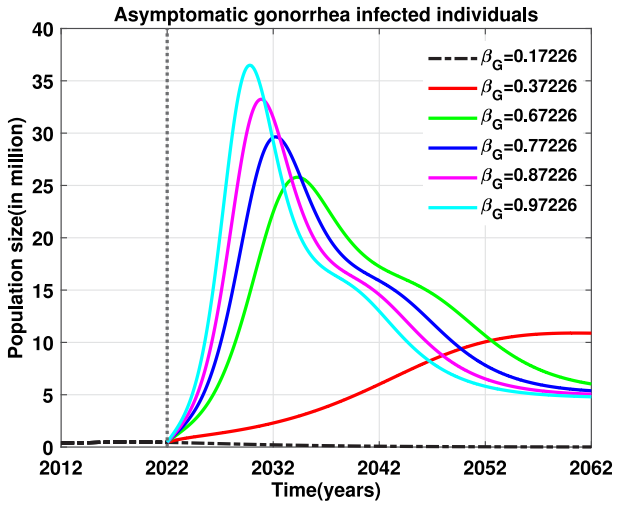

Fig. 18. Effect of varying β_G on $A_G(t)$. The vertical line indicates the end of the observed data period and the start of the predictive simulation.

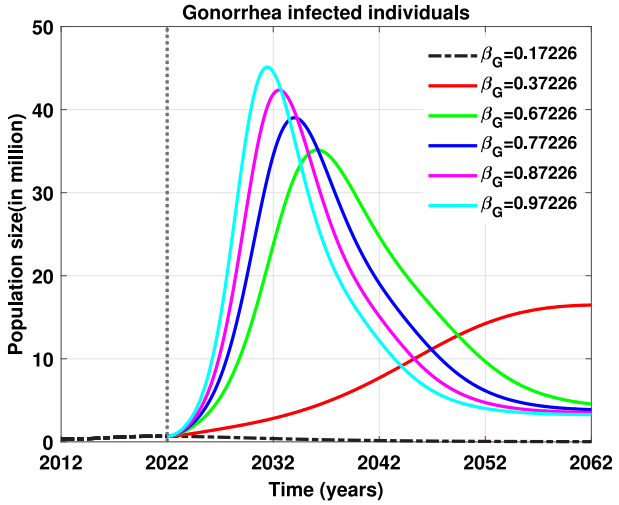

Fig. 19. Effect of varying β_G on $I_G(t)$. The vertical line indicates the end of the observed data period and the start of the predictive simulation.

and informing sexual partners can help further reduce co-infection rates. These preventive strategies are critical in controlling the spread of both infections, improving long-term health outcomes, and easing the burden on public health systems.

7.2. Influence of β_H on infected compartments

In this section, we predict the impact of varying the effective contact rate for HPV transmission β_H from 2022 to 2062, on different compartments in the model, specifically focusing on asymptomatic HPV infected individuals, symptomatic HPV infected individuals and those co-infected with both HPV and gonorrhea.

(i) **Effects of β_H on asymptomatic HPV infected individuals:** Fig. 21 illustrates the effect of varying β_H on the population of $A_H(t)$. As β_H decreases, there is a notable reduction in the number of asymptomatic HPV cases. This decrease is crucial because asymptomatic individuals, while not showing symptoms, still contribute to the spread of HPV within the community. Identifying and managing asymptomatic infections is vital to control the overall transmission of HPV. By lowering β_H, the model predicts a quicker decline in asymptomatic cases, ultimately aiding in the reduction of HPV spread among the population.

(ii) **Effects of β_H on symptomatic HPV infected individuals:** Fig. 22 shows the impact of β_H on $I_H(t)$. Similar to the asymptomatic compartment, reducing β_H leads to a significant decrease in the number of symptomatic cases over time.

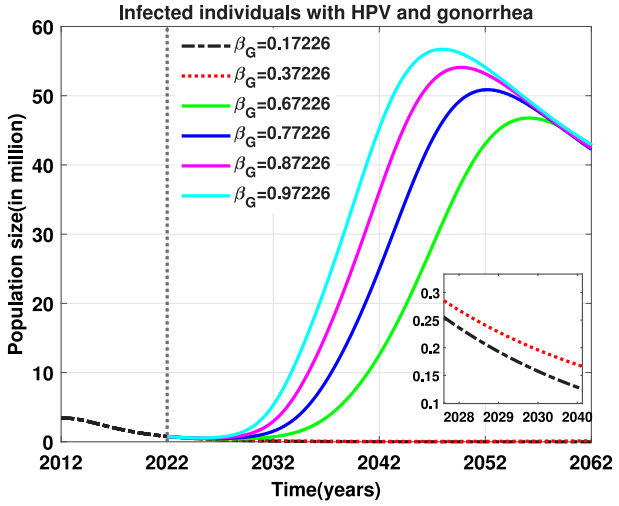

Fig. 20. Effect of varying β_G on $I_{HG}(t)$. The vertical line indicates the end of the observed data period and the start of the predictive simulation.

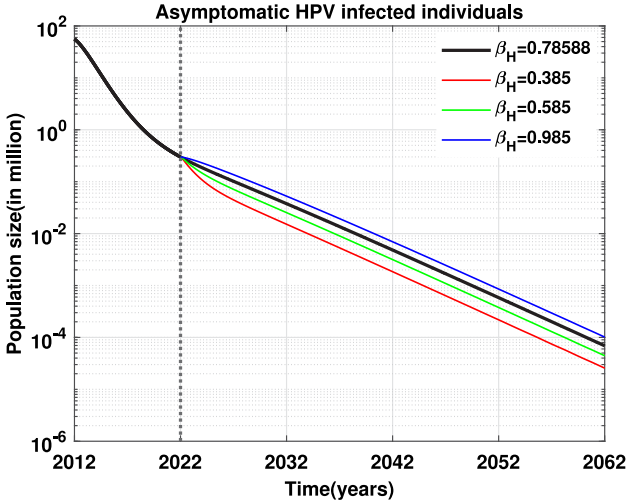

Fig. 21. Effect of varying β_H on $A_H(t)$. The vertical line indicates the end of the observed data period and the start of the predictive simulation.

Reducing the contact rate diminishes the severity of symptomatic HPV infections and expedites the reduction of its public health threat. By lowering β_H, the spread of the disease is minimized, leading to fewer symptomatic cases requiring attention.

(iii) **Effects of β_H on co-infected individuals:** The effect of β_H on the population of individuals co-infected with HPV and gonorrhea, $I_{HG}(t)$, is depicted in Fig. 23. Reducing β_H has a profound impact on the number of co-infected individuals, highlighting the interplay between HPV transmission and the risk of acquiring gonorrhea. As β_H decreases, not only does the incidence of co-infection diminish, but the overall risk of complications arising from dual infections is also mitigated. This underscores the importance of maintaining low transmission rates to prevent the spread of both HPV and gonorrhea.

Thus, reducing β_H is a key strategy in the fight against HPV, as it directly impacts the prevalence of both asymptomatic and symptomatic infections, as well as the number of co-infected individuals. A lower β_H leads to the quicker elimination of the disease from the community and reduces the maximum number of infections. Effective public health strategies should emphasize the importance of reducing contact rates, increasing awareness about asymptomatic infections and promoting behaviors that prevent HPV transmission. These measures combined with vaccination and timely medical intervention, are essential for reducing the incidence of HPV and its associated complications, ultimately leading to a healthier population.

8. Incorporation of control variables into the model

In the context of controlling the spread of HPV and gonorrhea co-infection, we introduce three time-dependent control variables: $u_1(t)$, $u_2(t)$ and $u_3(t)$ in the model (1). These controls are designed to address key aspects of disease prevention and management,

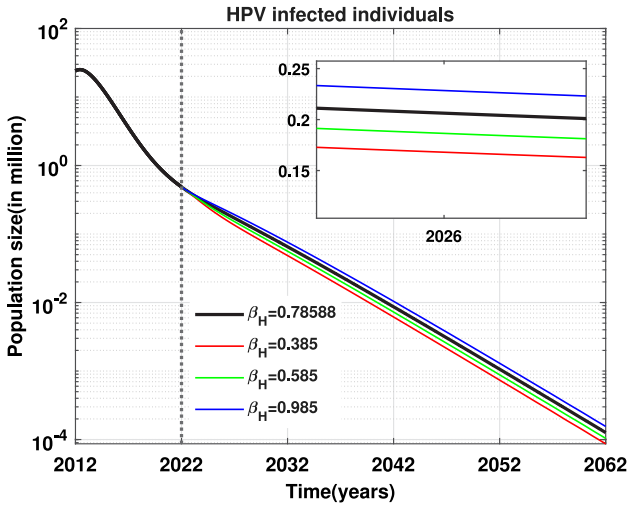

Fig. 22. Effect of varying β_H on $I_H(t)$. The vertical line indicates the end of the observed data period and the start of the predictive simulation.

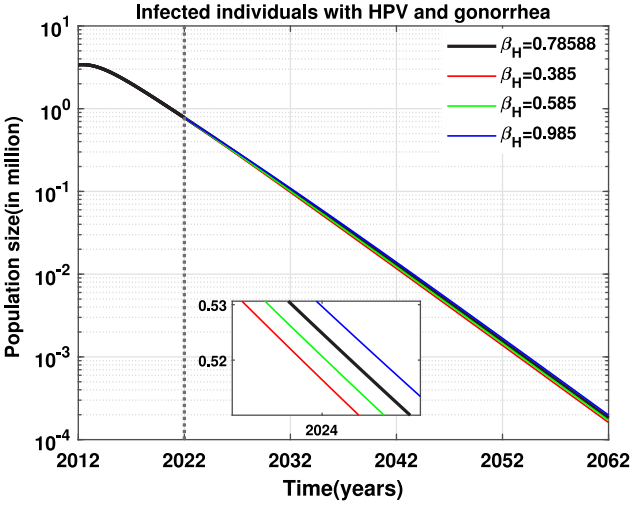

Fig. 23. Effect of varying β_H on $I_{HG}(t)$. The vertical line indicates the end of the observed data period and the start of the predictive simulation.

with the aim of reducing transmission and mitigating the impact of the infections. The first control variable $u_1(t)$ represents efforts to minimize contact between susceptible individuals and those infected with either HPV or gonorrhea. This can be achieved through educational campaigns that raise awareness about the modes of disease transmission and promote the use of condoms as a preventive measure. By educating the susceptible population and those already vaccinated against HPV, $u_1(t)$ seeks to reduce the probability of new infections by altering behavior and increasing the adoption of protective practices. The second control variable $u_2(t)$ corresponds to the variation in the vaccination rate. Although the vaccination rate is often assumed to be constant, by adjusting $u_2(t)$, we can evaluate the effectiveness of different vaccination strategies and determine the optimal level of effort required to maximize the benefits of vaccination programs in the population. The third control variable $u_3(t)$ is introduced to enhance the treatment of gonorrhea. This control reflects efforts to increase the availability and use of antibiotics for treating gonorrhea, as well as initiatives to raise awareness about the risks of reinfection and the importance of timely hospitalization. By intensifying treatment efforts, $u_3(t)$ aims to reduce the prevalence of gonorrhea, particularly among those co-infected with HPV, and to mitigate the overall burden of the disease.

The model with control variables is depicted in the schematic flow diagram shown in Fig. 24, which illustrates the flow of individuals through various population compartments while explicitly accounting for the influence of control measures. For convenience, we denote as u_1, u_2, u_3. Following the above discussion, the deterministic system of nonlinear differential equations

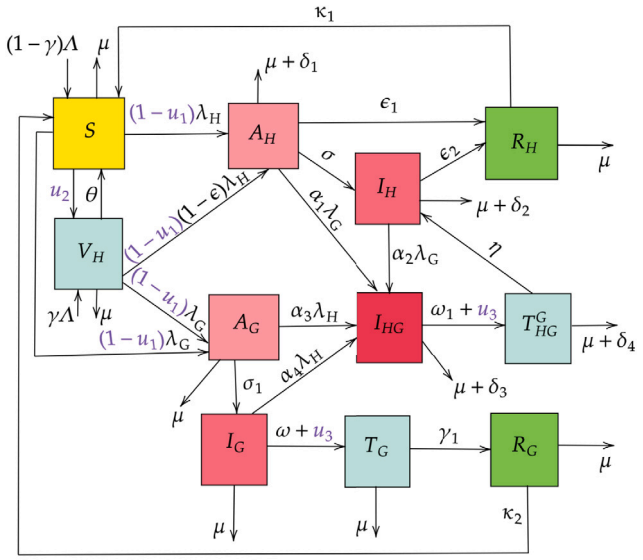

Fig. 24. Schematic flow diagram of HPV and gonorrhea co-infection model with control variables.

with control variables is formulated as follows:

$$
\begin{aligned}
\frac{dS}{dt} &= (1-\gamma)\Lambda - (1-u_1)\lambda_H S - (1-u_1)\lambda_G S + \theta V_H - (u_2+\mu)S + \kappa_1 R_H + \kappa_2 R_G,\\
\frac{dV_H}{dt} &= \gamma\Lambda + u_2 S - (1-u_1)(1-\epsilon)\lambda_H V_H - (1-u_1)\lambda_G V_H - (\theta+\mu)V_H,\\
\frac{dA_H}{dt} &= (1-u_1)\lambda_H S + (1-u_1)(1-\epsilon)\lambda_H V_H - \alpha_1\lambda_G A_H - (\sigma+\epsilon_1+\mu+\delta_1)A_H,\\
\frac{dI_H}{dt} &= \sigma A_H - \alpha_2\lambda_G I_H + \eta T^G_{HG} - (\epsilon_2+\mu+\delta_2)I_H,\\
\frac{dR_H}{dt} &= \epsilon_1 A_H + \epsilon_2 I_H - (\kappa_1+\mu)R_H,\\
\frac{dA_G}{dt} &= (1-u_1)\lambda_G V_H + (1-u_1)\lambda_G S - \alpha_3\lambda_H A_G - (\sigma_1+\mu)A_G,\\
\frac{dI_G}{dt} &= \sigma_1 A_G - \alpha_4\lambda_H I_G - (\omega+u_3+\mu)I_G,\\
\frac{dI_{HG}}{dt} &= (\alpha_1 A_H + \alpha_2 I_H)\lambda_G + (\alpha_3 A_G + \alpha_4 I_G)\lambda_H - (\omega_1+u_3+\mu+\delta_3)I_{HG},\\
\frac{dT_G}{dt} &= (\omega+u_3)I_G - (\gamma_1+\mu)T_G,\\
\frac{dT^G_{HG}}{dt} &= (\omega_1+u_3)I_{HG} - (\eta+\mu+\delta_4)T^G_{HG},\\
\frac{dR_G}{dt} &= \gamma_1 T_G - (\kappa_2+\mu)R_G,
\end{aligned}
\tag{8}
$$

with nonnegative initial conditions (2).

Here $N = S + V_H + A_H + I_H + R_H + A_G + I_G + I_{HG} + T_G + T^G_{HG} + R_G$, $\lambda_H = \dfrac{\beta_H(A_H + \psi_1 I_H + \psi_2 I_{HG} + \psi_3 T^G_{HG})}{N}$ and $\lambda_G = \dfrac{\beta_G(A_G + \phi_1 I_G + \phi_2 T_G + \phi_3 I_{HG} + \phi_4 T^G_{HG})}{N}$.

8.1. An optimal control problem

In this section, an optimal control problem is defined to identify the most effective strategies for mitigating the co-infection of HPV and gonorrhea, while minimizing the implementation costs. Our primary goal is to reduce the number of infected individuals in the compartments A_H, I_H, A_G, I_G, and I_{HG} along with minimizing the costs associated with the control measures. To achieve

this, the following objective functional is constructed:

$$\mathcal{J}(u) = \min_{u\in\mathcal{U}} \int_0^{t_f} a_1 A_H + a_2 I_H + a_3 A_G + a_4 I_G + a_5 I_{HG} + \frac{1}{2}(b_1 u_1^2 + b_2 u_2^2 + b_3 u_3^2)\, dt,$$

where t_f is the final time of the intervention period. $\mathcal{U}$ is the control set defined by

$$\mathcal{U} = \{(u_1, u_2, u_3) | u_i \text{ is Lebesgue measurable, } 0 \le u_i(t) \le u_{i_{\max}} < 1, t \in [0, t_f], i = 1, 2, 3\},$$

with $u_{1_{\max}} = 0.8$, $u_{2_{\max}} = 0.9$, and $u_{3_{\max}} = 0.9$. Since preventive measures, time-varying vaccination and enhanced gonorrhea treatment may not achieve perfect efficiency in real-world scenarios, the values of $u_{i_{\max}}$ are set to be strictly less than 1. Here a_i $(i = 1, 2, \dots, 5)$ and b_i $(i = 1, 2, 3)$ are positive weight constants associated with the infected compartments and the control efforts respectively. The term $a_1 A_H(t) + a_2 I_H(t) + a_3 A_G(t) + a_4 I_G(t) + a_5 I_{HG}(t)$ represents the cost attributed to treat infected individuals, while $\frac{1}{2}(b_1 u_1^2(t) + b_2 u_2^2(t) + b_3 u_3^2(t))$ accounts for the costs associated with the respective control measures.

8.2. Existence of an optimal control

Theorem 8.1. *Given the objective functional $\mathcal{J}(u)$ subject to the system (8) defined on $\mathcal{U}$ with the nonnegative initial conditions (2), then there exists an optimal control $u^* = (u_1^*, u_2^*, u_3^*)$ and their corresponding optimal state variables $X^*(t) = (S^*, V_H^*, A_H^*, I_H^*, R_H^*, A_G^*, I_G^*, I_{HG}^*, T_G^*, T_{HG}^{G^*}, R_G^*)$ such that*

$$\mathcal{J}(u^*) = \min_{u\in\mathcal{U}} \mathcal{J}(u)$$

if the following conditions hold:

- *(i) The set of solutions to the co-infection model with initial conditions and the associated control variables in $\mathcal{U}$ are non-empty.*
- *(ii) The admissible control set $\mathcal{U}$ is convex and closed.*
- *(iii) The function $f(t, X, u)$ representing the right side of the system (8) is continuous and can be expressed as $f(t, X, u) = f_1(t, X) + f_2(t, X)(u_1, u_2, u_3)^\top$.*
- *(iv) The integrand of the objective functional $\mathcal{L}(X, u)$ is convex on $\mathcal{U}$.*
- *(v) There exist constants $C_1, C_2 > 0$ and $\kappa > 1$ such that $\mathcal{L}(X, u) \ge C_1(|u|^2)^{\kappa/2} - C_2$, where $\mathcal{L}(X, u) = a_1 A_H + a_2 I_H + a_3 A_G + a_4 I_G + a_5 I_{HG} + \frac{1}{2}(b_1 u_1^2 + b_2 u_2^2 + b_3 u_3^2)$ and $|u| = \sqrt{u_1^2 + u_2^2 + u_3^2}$.*

Proof. The central idea behind this proof is drawn from the theorem established by Fleming and Rishel in [54].

(i) The techniques presented in [55,56] are utilized to establish (i). Since $X(t) \in \Xi_3$, all state variables are bounded, ensuring that the solutions to the state equations are also bounded. The boundedness of the partial derivatives with respect to the state variables confirms the Lipschitz continuity of the system with respect to these variables. Consequently, a solution to the system (8) exists for each admissible control in $\mathcal{U}$.

(ii) By definition of the control set, it can be written as $\mathcal{U} = U_1 \times U_2 \times U_3$.
Here, $U_1 = \{u_1 | u_1 \text{ is Lebesgue measurable, } 0 \le u_1(t) \le u_{1_{\max}} < 1, t \in [0, t_f]\}$ and similarly define for U_2 and U_3. It is obvious that each U_i is closed, thus $\mathcal{U}$ is closed. Now to prove U_1 is convex. Take the functions h_1 and h_2 from the set U_1. By the properties of Lebesgue measurable functions, it is clear that $ah_1 + (1-a)h_2$ is also Lebesgue measurable for $a \in [0, 1]$. Hence $ah_1 + (1-a)h_2 \in U_1$, proving U_1 is convex. Similar arguments hold for U_2 and U_3. Thus $\mathcal{U}$ is convex.

(iii) It is explicit that $f(t, X, u)$ is continuous. Also, it can be rewritten as

$$f(t, X, u) = f_1(t, X) + f_2(t, X)(u_1, u_2, u_3)^\top,$$

which is linearly dependent on controls u_1, u_2 and u_3. Here,

$$f_1(t, X) = \begin{bmatrix} (1-\gamma)\Lambda - \lambda_H S - \lambda_G S + \theta V_H - \mu S + \kappa_1 R_H + \kappa_2 R_G \\ \gamma\Lambda - (1-\epsilon)\lambda_H V_H - \lambda_G V_H - (\theta + \mu)V_H \\ \lambda_H S + (1-\epsilon)\lambda_H V_H - \alpha_1 \lambda_G A_H - (\sigma + \epsilon_1 + \mu + \delta_1)A_H \\ \sigma A_H - \alpha_2 \lambda_G I_H + \eta T_{HG}^G - (\epsilon_2 + \mu + \delta_2)I_H \\ \epsilon_1 A_H + \epsilon_2 I_H - (\kappa_1 + \mu)R_H \\ \lambda_G V_H + \lambda_G S - \alpha_3 \lambda_H A_G - (\sigma_1 + \mu)A_G \\ \sigma_1 A_G - \alpha_4 \lambda_H I_G - (\omega + \mu)I_G \\ (\alpha_1 A_H + \alpha_2 I_H)\lambda_G + (\alpha_3 A_G + \alpha_4 I_G)\lambda_H - (\omega_1 + \mu + \delta_3)I_{HG} \\ \omega I_G - (\gamma_1 + \mu)T_G \\ \omega_1 I_{HG} - (\eta + \mu + \delta_4)T_{HG}^G \\ \gamma_1 T_G - (\kappa_2 + \mu)R_G \end{bmatrix} \text{ and}$$

$$f_2(t,X)=\begin{bmatrix}(\lambda_H+\lambda_G)S & -S & 0\\ ((1-\epsilon)\lambda_H+\lambda_G)V_H & S & 0\\ -(S+(1-\epsilon)V_H)\lambda_H & 0 & 0\\ 0 & 0 & 0\\ 0 & 0 & 0\\ -(\lambda_G V_H+\lambda_G S) & 0 & 0\\ 0 & 0 & -I_G\\ 0 & 0 & -I_{HG}\\ 0 & 0 & I_G\\ 0 & 0 & I_{HG}\\ 0 & 0 & 0\end{bmatrix}.$$

(iv) To prove that $\mathcal{L}(X,u)$ is convex on $\mathcal{U}$, we need to show that for any $p,q\in\mathcal{U}$ and $a\in[0,1]$, the following inequality holds:

$$\mathcal{L}(X,(1-a)p+aq)\le(1-a)\mathcal{L}(X,p)+a\mathcal{L}(X,q).$$

Claim: $\mathbb{L}=\mathcal{L}(X,(1-a)p+aq)-(1-a)\mathcal{L}(X,p)-a\mathcal{L}(X,q)\le 0.$

$$\begin{aligned}\text{Now, } \mathbb{L}&=\mathcal{L}(X,(1-a)p_1+aq_1,(1-a)p_2+aq_2,(1-a)p_3+aq_3)-(1-a)\mathcal{L}(X,p_1,p_2,p_3)-a\mathcal{L}(X,q_1,q_2,q_3),\\ &=a_1A_H+a_2I_H+a_3A_G+a_4I_G+a_5I_{HG}\\ &\quad+\frac{1}{2}(b_1((1-a)p_1+aq_1)^2+b_2((1-a)p_2+aq_2)^2+b_3((1-a)p_3+aq_3)^2)\\ &\quad-(1-a)(a_1A_H+a_2I_H+a_3A_G+a_4I_G+a_5I_{HG}+\frac{1}{2}(b_1p_1^2+b_2p_2^2+b_3p_3^2))\\ &\quad-a(a_1A_H+a_2I_H+a_3A_G+a_4I_G+a_5I_{HG}+\frac{1}{2}(b_1q_1^2+b_2q_2^2+b_3q_3^2)),\\ &=\frac{a(a-1)}{2}(b_1(p_1-q_1)^2+b_2(p_2-q_2)^2+b_3(p_3-q_3)^2),\\ &\le 0,\ \text{ since }\ a-1\le 0.\end{aligned}$$

Hence, $\mathcal{L}(X,u)$ is convex on $\mathcal{U}$.

(v) Consider

$$\begin{aligned}\mathcal{L}(X,u)&=a_1A_H+a_2I_H+a_3A_G+a_4I_G+a_5I_{HG}+\frac{1}{2}(b_1u_1^2+b_2u_2^2+b_3u_3^2),\\ &\ge\frac{1}{2}(b_1u_1^2+b_2u_2^2+b_3u_3^2),\\ &\ge C_1(u_1^2+u_2^2+u_3^2)-C_2,\ \text{ where } C_1=\min\left\{\frac{b_1}{2},\frac{b_2}{2},\frac{b_3}{2}\right\}\text{ and } C_2>0.\end{aligned}$$

Therefore, $\mathcal{L}(X,u)\ge C_1(|u|^2)^{\kappa/2}-C_2$, where $\kappa=2>1, C_1>0$ and $C_2>0$.

Thus an optimal control $u^*\in\mathcal{U}$ exists, such that $\mathcal{J}(u^*)=\min_{u\in\mathcal{U}}\mathcal{J}(u)$. □

8.3. Necessary conditions for an optimality system

Let us define Lagrangian $\mathcal{L}$ and Hamiltonian $\mathcal{H}$ as follows:

$$\mathcal{L}(X,u)=a_1A_H+a_2I_H+a_3A_G+a_4I_G+a_5I_{HG}+\frac{1}{2}(b_1u_1^2+b_2u_2^2+b_3u_3^2),$$

and

$$\begin{aligned}\mathcal{H}(X,u,\lambda)&=\mathcal{L}(X,u)+\lambda_1((1-\gamma)\Lambda-(1-u_1)\lambda_HS-(1-u_1)\lambda_GS+\theta V_H-(u_2+\mu)S+\kappa_1R_H+\kappa_2R_G)\\ &\quad+\lambda_2(\gamma\Lambda+u_2S-(1-u_1)(1-\epsilon)\lambda_HV_H-(1-u_1)\lambda_GV_H-(\theta+\mu)V_H)\\ &\quad+\lambda_3((1-u_1)\lambda_HS+(1-u_1)(1-\epsilon)\lambda_HV_H-\alpha_1\lambda_GA_H-(\sigma+\epsilon_1+\mu+\delta_1)A_H)\\ &\quad+\lambda_4(\sigma A_H-\alpha_2\lambda_GI_H+\eta T_{HG}^G-(\epsilon_2+\mu+\delta_2)I_H)\\ &\quad+\lambda_5(\epsilon_1A_H+\epsilon_2I_H-(\kappa_1+\mu)R_H)\\ &\quad+\lambda_6((1-u_1)\lambda_GV_H+(1-u_1)\lambda_GS-\alpha_3\lambda_HA_H-(\sigma_1+\mu)A_G)\\ &\quad+\lambda_7(\sigma_1A_G-\alpha_4\lambda_HI_G-(\omega+u_3+\mu)I_G)\\ &\quad+\lambda_8((\alpha_1A_H+\alpha_2I_H)\lambda_G+(\alpha_3A_G+\alpha_4I_G)\lambda_H-(\omega_1+u_3+\mu+\delta_3)I_{HG})\\ &\quad+\lambda_9((\omega+u_3)I_G-(\gamma_1+\mu)T_G)\\ &\quad+\lambda_{10}((\omega_1+u_3)I_{HG}-(\eta+\mu+\delta_4)T_{HG}^G)\\ &\quad+\lambda_{11}(\gamma_1T_G-(\kappa_2+\mu)R_G).\end{aligned}\tag{9}$$

Here $\lambda(t)=(\lambda_i(t)), i=1,2,\dots,11$. The elements of $\lambda(t)$ are called adjoint variables corresponding to the state variables $X(t)$.

Theorem 8.2. *Let u^* be an optimal control with X^* as the optimal solutions of the system (8) that minimizes $\mathcal{J}(u^*)$ over the control set $\mathcal{U}$, then there exist adjoint variables λ_i $(i = 1, 2, \dots, 11)$ satisfying*

$$
\begin{aligned}
\frac{d\lambda_1}{dt} &= \mu\lambda_1 - (\lambda_2 - \lambda_1)u_2^* - (\lambda_H^*/N^*)((1-u_1^*)N^*(\lambda_3 - \lambda_1) + Y^*) - (\lambda_G^*/N^*)((1-u_1^*)N^*(\lambda_6 - \lambda_1) + Z^*),\\
\frac{d\lambda_2}{dt} &= \mu\lambda_2 - (\lambda_1 - \lambda_2)\theta - (\lambda_H^*/N^*)((1-u_1^*)(1-\epsilon)N^*(\lambda_3 - \lambda_2) + Y^*) - (\lambda_G^*/N^*)((1-u_1^*)N^*(\lambda_6 - \lambda_2) + Z^*),\\
\frac{d\lambda_3}{dt} &= -a_1 + (\mu + \delta_1)\lambda_3 - (\lambda_5 - \lambda_3)\epsilon_1 - (\lambda_4 - \lambda_3)\sigma + (\beta_H - \lambda_H^*)(Y^*/N^*) - (\lambda_G^*/N^*)((\lambda_8 - \lambda_3)\alpha_1 N^* + Z^*),\\
\frac{d\lambda_4}{dt} &= -a_2 + (\mu + \delta_2)\lambda_4 - (\lambda_5 - \lambda_4)\epsilon_2 + (\beta_H\psi_1 - \lambda_H^*)(Y^*/N^*) - (\lambda_G^*/N^*)((\lambda_8 - \lambda_4)\alpha_2 N^* + Z^*),\\
\frac{d\lambda_5}{dt} &= \mu\lambda_5 - (\lambda_1 - \lambda_5)\kappa_1 - (\lambda_H^* Y^*/N^*) - (\lambda_G^* Z^*/N^*),\\
\frac{d\lambda_6}{dt} &= -a_3 + \mu\lambda_6 - (\lambda_7 - \lambda_6)\sigma_1 - (\lambda_H^*/N^*)(\alpha_3 N^*(\lambda_8 - \lambda_6) + Y^*) + (\beta_G - \lambda_G^*)(Z^*/N^*),\\
\frac{d\lambda_7}{dt} &= -a_4 + \mu\lambda_7 - (\lambda_9 - \lambda_7)(\omega + u_3^*) - (\lambda_H^*/N^*)(\alpha_4 N^*(\lambda_8 - \lambda_7) + Y^*) + (\beta_G\phi_1 - \lambda_G^*)(Z^*/N^*),\\
\frac{d\lambda_8}{dt} &= -a_5 + (\mu + \delta_3)\lambda_8 - (\lambda_{10} - \lambda_8)(\omega_1 + u_3^*) + (\beta_H\psi_2 - \lambda_H^*)(Y^*/N^*) + (\beta_G\phi_3 - \lambda_G^*)(Z^*/N^*),\\
\frac{d\lambda_9}{dt} &= \mu\lambda_9 - (\lambda_{11} - \lambda_9)\gamma_1 - (\lambda_H^* Y^*/N^*) + (\beta_G\phi_2 - \lambda_G^*)(Z^*/N^*),\\
\frac{d\lambda_{10}}{dt} &= (\mu + \delta_4)\lambda_{10} - (\lambda_4 - \lambda_{10})\eta + (\beta_H\psi_3 - \lambda_H^*)(Y^*/N^*) + (\beta_G\phi_4 - \lambda_G^*)(Z^*/N^*),\\
\frac{d\lambda_{11}}{dt} &= \mu\lambda_{11} - (\lambda_1 - \lambda_{11})\kappa_2 - (\lambda_H^* Y^*/N^*) - (\lambda_G^* Z^*/N^*),
\end{aligned}
\tag{10}
$$

where, $Y^* = (1-u_1^*)((\lambda_1 - \lambda_3)S^* + (1-\epsilon)(\lambda_2 - \lambda_3)V_H^*) + \alpha_3(\lambda_6 - \lambda_8)A_G^* + \alpha_4(\lambda_7 - \lambda_8)I_G^*$,

and $Z^* = (1-u_1^*)((\lambda_1 - \lambda_6)S^* + (\lambda_2 - \lambda_6)V_H^*) + \alpha_1(\lambda_3 - \lambda_8)A_H^* + \alpha_2(\lambda_4 - \lambda_8)I_H^*$,

along with transversality conditions:

$$\lambda_i(t_f) = 0, \quad i = 1, 2, \dots, 11. \tag{11}$$

And, optimal controls are characterized by

$$
\begin{aligned}
u_1^* &= \min\left\{u_{1_{\max}}, \max\left\{0, \frac{\lambda_H^*\left((\lambda_3 - \lambda_1)S^* + (\lambda_3 - \lambda_2)(1-\epsilon)V_H^*\right) + \lambda_G^*\left((\lambda_6 - \lambda_1)S^* + (\lambda_6 - \lambda_2)V_H^*\right)}{b_1}\right\}\right\},\\
u_2^* &= \min\left\{u_{2_{\max}}, \max\left\{0, \frac{(\lambda_1 - \lambda_2)S^*}{b_2}\right\}\right\},\\
u_3^* &= \min\left\{u_{3_{\max}}, \max\left\{0, \frac{(\lambda_7 - \lambda_9)I_G^* + (\lambda_8 - \lambda_{10})I_{HG}^*}{b_3}\right\}\right\}.
\end{aligned}
$$

Here, λ_G^*, λ_H^* and N^* represent the values of λ_G, λ_H and N, respectively, at the optimal states.

Proof. The well established Pontryagin's minimum principle [57] has been applied to establish the necessary conditions for the optimality system. The adjoint equations can be derived by computing the negative partial derivative of the Hamiltonian function (9) with respect to each state variables, resulting in (10). Since all the state variables are unrestricted at the terminal time, the transversality conditions is obtained as specified in (11).

To characterize the optimal controls, the optimality conditions can be derived by using,

$$\frac{\partial\mathcal{H}}{\partial u_i} = 0 \text{ at } u_i = u_i^*, i = 1, 2, 3. \tag{12}$$

Thus,

$$
\begin{aligned}
\left.\frac{\partial\mathcal{H}}{\partial u_1}\right|_{u_1 = u_1^*} &= \lambda_H((\lambda_1 - \lambda_3)S + (\lambda_2 - \lambda_3)(1-\epsilon)V_H) + \lambda_G((\lambda_1 - \lambda_6)S + (\lambda_2 - \lambda_6)V_H) + b_1 u_1^*,\\
\left.\frac{\partial\mathcal{H}}{\partial u_2}\right|_{u_2 = u_2^*} &= (\lambda_2 - \lambda_1)S + b_2 u_2^*,\\
\left.\frac{\partial\mathcal{H}}{\partial u_3}\right|_{u_3 = u_3^*} &= (\lambda_9 - \lambda_7)I_G + (\lambda_{10} - \lambda_8)I_{HG} + b_3 u_3^*.
\end{aligned}
$$

Using (12), the optimal controls are found as follows:

$$u_1^* = \frac{\lambda_H((\lambda_3 - \lambda_1)S + (\lambda_3 - \lambda_2)(1-\epsilon)V_H) + \lambda_G((\lambda_6 - \lambda_1)S + (\lambda_6 - \lambda_2)V_H)}{b_1},$$

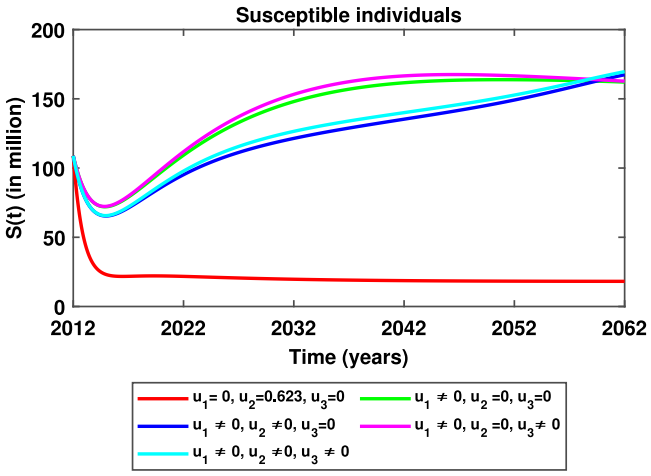

Fig. 25. Effects of various control strategies on $S(t)$.

$$u_2^* = \frac{(\lambda_1 - \lambda_2)S}{b_2},$$
$$u_3^* = \frac{(\lambda_7 - \lambda_9)I_G + (\lambda_8 - \lambda_{10})I_{HG}}{b_3}.$$

Since the controls are bounded, the optimal controls are characterized as

$$u_1^* = \min\left\{u_{1_{\max}}, \max\left\{0, \frac{\lambda_H^*\left((\lambda_3 - \lambda_1)S^* + (\lambda_3 - \lambda_2)(1-\epsilon)V_H^*\right)}{b_1} + \frac{\lambda_G^*\left((\lambda_6 - \lambda_1)S^* + (\lambda_6 - \lambda_2)V_H^*\right)}{b_1}\right\}\right\},$$
$$u_2^* = \min\left\{u_{2_{\max}}, \max\left\{0, \frac{(\lambda_1 - \lambda_2)S^*}{b_2}\right\}\right\},$$
$$u_3^* = \min\left\{u_{3_{\max}}, \max\left\{0, \frac{(\lambda_7 - \lambda_9)I_G^* + (\lambda_8 - \lambda_{10})I_{HG}^*}{b_3}\right\}\right\}. \quad \square$$

8.4. Dynamics of the model with control strategies

Given the critical importance of implementing effective control measures, we aim to study the behavior of different population groups within the model, including susceptible individuals, the total HPV infected population, the total gonorrhea infected population and the co-infected individuals. To evaluate the effectiveness of various intervention strategies, we propose four distinct approaches, all of which include the control measure u_1 (educational campaigns and awareness) as active ($u_1 \neq 0$) due to its significance in preventing STI spread. The strategies are as follows:

(i) **Strategy A:** $u_1 \neq 0$, $u_2 = 0$, $u_3 = 0$.
(ii) **Strategy B:** $u_1 \neq 0$, $u_2 = 0$, $u_3 \neq 0$.
(iii) **Strategy C:** $u_1 \neq 0$, $u_2 \neq 0$, $u_3 = 0$.
(iv) **Strategy D:** $u_1 \neq 0$, $u_2 \neq 0$, $u_3 \neq 0$.

8.4.1. Impact of different strategies on $S(t)$

Fig. 25 shows the impact of the different strategies on the susceptible population and highlights the effectiveness of the proposed approaches in preventing the spread of HPV and gonorrhea. Notably, without any additional control measures, the susceptible population exhibits a decreasing trend, indicating an increasing rate of infection over time. Strategy A, which focuses solely on educational campaigns and awareness ($u_1 \neq 0$, $u_2 = 0$, $u_3 = 0$), is effective in reducing the number of new infections compared to the uncontrolled scenario. However, strategy B, which combines educational campaigns with improved gonorrhea treatment ($u_1 \neq 0$, $u_2 = 0$, $u_3 \neq 0$), provides greater protection for the susceptible population, as evidenced by a higher proportion of susceptible individuals. Strategy C incorporates both educational campaigns and vaccination ($u_1 \neq 0$, $u_2 \neq 0$, $u_3 = 0$), whereas strategy D utilizes all three control measures, including enhanced gonorrhea treatment ($u_1 \neq 0$, $u_2 \neq 0$, $u_3 \neq 0$). When comparing these two strategies, strategy D is more effective in preventing infections, as reflected by a higher number of susceptible in the population. This outcome demonstrates the benefit of a comprehensive approach that integrates awareness, vaccination and treatment. It is important to note that the lower levels of susceptible observed in strategies C and D compared to strategies A and B are due to the inclusion of vaccination in the former strategies. Vaccination reduces the number of susceptible by moving individuals into the

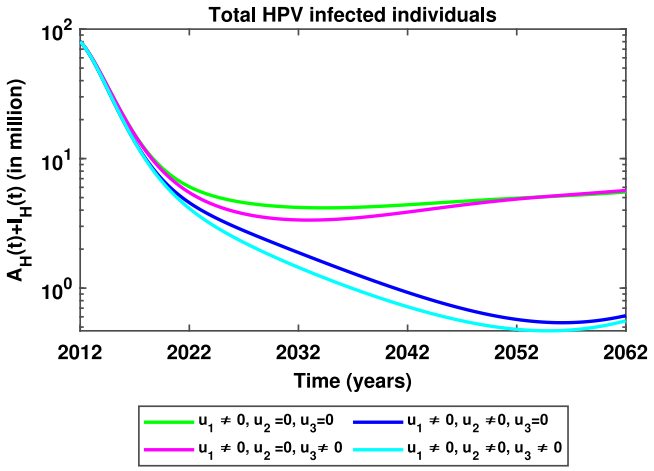

Fig. 26. Effects of various control strategies on the total number of HPV infected individuals.

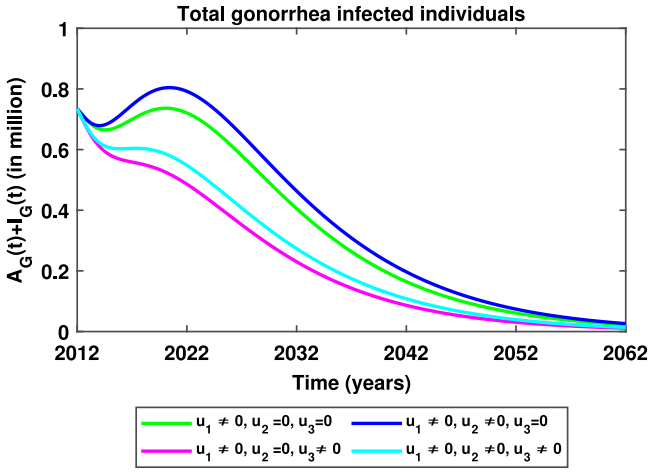

Fig. 27. Effects of various control strategies on the total number of gonorrhea infected individuals.

vaccinated compartment, thereby making direct comparisons between all strategies less straightforward. Thus effectiveness should be understood within the context of its specific interventions.

8.4.2. Effects of various control strategies on the total number of HPV infected individuals

To better understand the impact of different control strategies on the total number of HPV infected individuals, we present the results in Fig. 26. This figure shows the combined population of asymptomatic and symptomatic HPV infected individuals, $A_H(t) + I_H(t)$, under various strategies. The impact of a time-varying vaccination rate is particularly evident in the results. Strategy A relies solely on educational campaigns without vaccination, results in the highest number of HPV infected individuals. Strategy B includes enhanced gonorrhea treatment but no vaccination, shows a slight reduction in HPV infections compared to strategy A. However, strategies C and D demonstrate a significant decrease in HPV infections, with strategy D being the most effective. The inclusion of a vaccination effort directly influences the outcomes, as the number of HPV infected individuals approach towards zero in strategies C and D. This contrasts with strategies A and B, where infections do not reach zero due to the absence of vaccination. Overall, the results highlight the critical role of vaccination in reducing HPV infections and demonstrate that the comprehensive implementation of all control measures is the most effective approach in lowering the total number of HPV infected individuals.

8.4.3. Impact of different strategies on the total number of gonorrhea infected individuals

To illustrate the impact of various control strategies on the total number of gonorrhea infected individuals, Fig. 27 visualizes the combined sum of asymptomatic and symptomatic gonorrhea cases, $A_G(t) + I_G(t)$, under different strategies. When comparing strategy A and strategy B, it is evident that strategy B yields a more significant reduction in the total number of gonorrhea infected individuals. Both strategies involve educational campaigns and awareness (with no vaccination efforts), but strategy B additionally

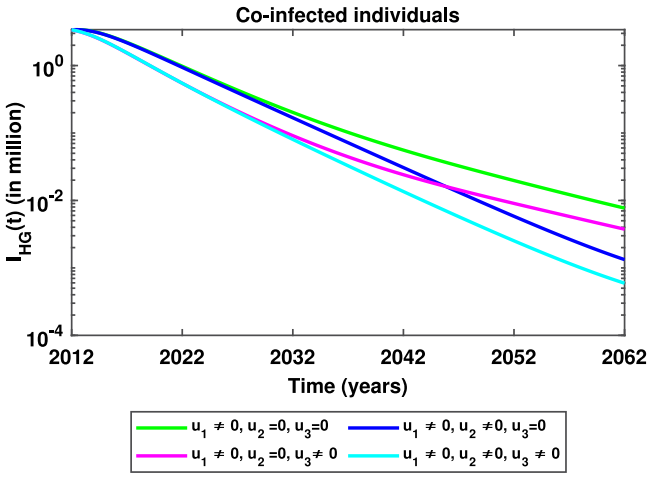

Fig. 28. Effects of various control strategies on co-infected individuals.

incorporates enhanced treatment for gonorrhea. The results indicate that the combination of prevention through education and targeted treatment significantly reduces the overall burden of gonorrhea in the population. When focusing on the strategies that incorporate vaccination efforts namely, strategy C and strategy D, it becomes evident that strategy D yields a more pronounced reduction in the total gonorrhea infected population compared to strategy C. This improved outcome is attributed to the inclusion of enhanced gonorrhea treatment alongside preventive measures such as public health education and time-dependent HPV vaccination.

8.4.4. Impact of different strategies on co-infected individuals

The impact of various strategies on the population of co-infected individuals is illustrated in Fig. 28. This figure shows that strategy D is the most effective in reducing the number of individuals co-infected with both HPV and gonorrhea. Strategy A results in the highest number of co-infected individuals throughout the entire period, indicating that relying solely on educational campaigns without vaccination or enhanced treatment is less efficient to control the co-infection situations. Strategy B initially shows a decreasing trend in co-infections, but after 2046, the absence of vaccination leads to an increase in co-infected individuals. This suggests that while strategy B may be effective in the short term, it is not sustainable for long-term control of co-infections. Strategy C starts with a slower decrease in co-infections, but eventually outperforms strategy B as time progresses. This is due to the combined effect of preventing susceptible from becoming infected and vaccinating them against HPV, alongside ongoing gonorrhea treatment. Overall, the analysis highlights the importance of a comprehensive approach that includes prevention, HPV vaccination, and enhanced gonorrhea treatment to effectively reduce the number of co-infected individuals over the long term.

8.4.5. The control profiles

To evaluate the effectiveness of the implemented control strategies in reducing the transmission of HPV and gonorrhea, the corresponding control profiles are elaborated in the subsequent discussion.

(i) Fig. 29 shows the profile of $u_1(t)$ representing educational campaigns focused on raising awareness and promoting condom use. It is observed that in strategies A and B, u_1 initially decreases but as infection spreads, the need for prevention grows which leads to a peak. Notably, towards the end of the intervention, it decreases again that indicates reduced effort as infections begin to decline. This emphasizes the importance of sustained educational efforts in controlling HPV and gonorrhea. In contrast, u_1 in strategies C and D shows a steady decline, approaching zero by the end of the intervention, suggesting that the additional measures in these strategies reduce the need for u_1.

(ii) Fig. 30 presents the control profile for $u_2(t)$, the time-dependent vaccination rate. In strategies C and D, u_2 shows an initial decrease followed by a steady level for approximately 30 years, reflecting a strategic approach to resource allocation. This sustained vaccination effort highlights the importance of managing vaccination resources based on infection dynamics. The effectiveness of this control is evident in the reduction of both single and co-infections.

(iii) Fig. 31 depicts the control profile for $u_3(t)$, which focuses on enhanced gonorrhea treatment. The figure shows that the required effort for u_3 is high at the beginning (in strategies B and D) and gradually decreases as the control measures take effect. This trend highlights the importance of early and intensive treatment interventions in managing both single infections and co-infections.

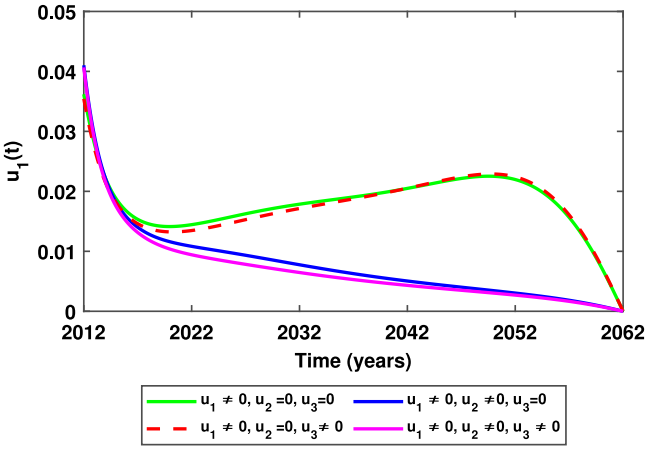

Fig. 29. Control profile of various control strategies on $u_1(t)$.

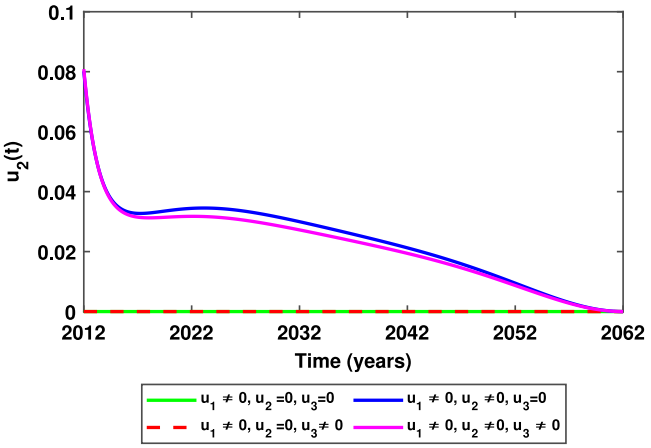

Fig. 30. Control profile of various control strategies on $u_2(t)$.

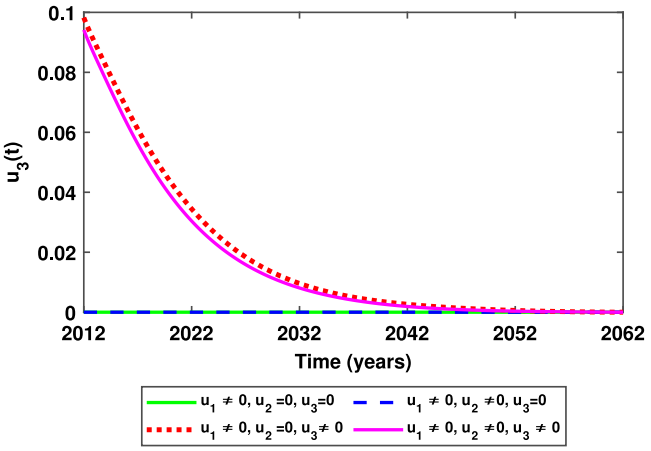

Fig. 31. Control profile of various control strategies on $u_3(t)$.

8.4.6. Practical implications of control strategies

Drawing from the optimal control results presented earlier, this subsection underscores the practical significance of time-dependent intervention strategies in managing HPV, gonorrhea, and their co-infection. A notable insight is the dynamical role

of educational campaigns depending on the broader intervention context. In scenarios where education serves as the primary control strategy, efforts increase as infections rise, reflecting the need to promote awareness and safer sexual behaviors. These efforts are sustained until infection levels begin to decrease. However, when educational campaigns are implemented alongside vaccination and treatment, their intensity significantly decreases over time, as the presence of these other effective interventions alleviates the burden on education-focused strategies. Specifically, HPV vaccination control reveals that an early scale-up and sustained coverage significantly lowers HPV prevalence over time. In fact, the interventions with vaccination nearly eliminate HPV infections, aligning with WHO's guidance on routine vaccination for adolescents as a core preventive measure. On the other hand, enhancing the gonorrhea treatment reflects the importance of quickly treating infected individuals to halt transmission, particularly in populations with higher infectivity, such as those who are co-infected with both gonorrhea and HPV. The initial treatment helps limit further spread, while tapering off over time ensures that resources are allocated efficiently without overburdening the healthcare system. Furthermore, simulation outcomes clearly indicate that a combined approach involving educational campaigns, HPV vaccination, and gonorrhea treatment are essential for achieving lasting reductions in both HPV and gonorrhea transmission, ultimately preventing co-infection and its associated public health burden.

9. Conclusion

In this study, a novel mathematical model that captures the dynamics of HPV and gonorrhea co-infection is proposed. We have established basic qualitative properties of the co-infection model, such as nonnegativity and boundedness of the solutions. The basic reproduction number ($\mathcal{R}_0$) is calculated using the next generation matrix method and stability analysis of disease-free equilibrium point is also performed on the proposed model. Boundary equilibria for the model is also derived. Then, the model is calibrated and validated with real-world gonorrhea infection data from the U.S., ensuring its accuracy and relevance to current epidemiological trends. Sensitivity analysis indicated that $\mathcal{R}_0$ is particularly more sensitive to the effective transmission rates of both HPV (β_H) and gonorrhea (β_G), identifying these rates as critical targets for intervention. Numerical simulations demonstrated that lowering β_H and β_G substantially reduces the number of co-infected individuals, thereby decreasing the overall risk of complications associated with dual infections. The obtained graphical results suggest that effective public health strategies should focus on reducing contact rates, raising awareness about asymptomatic infections and promoting preventive behaviors. These strategies combined with vaccination and timely medical intervention are essential for mitigating both HPV and gonorrhea.

Further, to mitigate the transmission of these infections, the three time-dependent control variables such as promoting safe sex practices, implementing a time-varying HPV vaccination rate and enhancing gonorrhea treatment are incorporated into the model. An optimal control problem is formulated to minimize the total number of infected individuals across various compartments and to reduce associated costs. The existence of an optimal control is established and the explicit analytical expressions for all the control variables are derived using Pontryagin's minimum principle. Numerical simulations using the Runge–Kutta forward–backward sweep method validated the analytical results and examined the effectiveness of the control strategies. The obtained results suggest that the simultaneous implementation of all control measures can significantly lower both single and co-infection rates, leading to improved public health outcomes. Furthermore, the insights gained from the findings provide valuable guidance for policymakers in formulating effective strategies to manage and mitigate the incidence of HPV and gonorrhea co-infections.

While the study presents important contributions to understanding the dynamics of these co-infections, certain limitations should be acknowledged as they point to the promising directions for future research. Notably, the current model does not incorporate sex-structured compartments, which limits its ability to capture the biological and behavioral differences in transmission and disease progression between males and females. Additionally, long-term health consequences of persistent HPV infection such as cervical, anal, and penile cancers are not explicitly modeled, limiting the ability to fully capture the broader health burden. Future models could be enhanced by including sex-specific dynamics and explicitly simulating the progression to cancer-related outcomes. Moreover, the existence of the interior (co-infection) endemic equilibrium remains analytically intractable due to the nonlinear structure of the system. Though the present study suggests the potential occurrence of backward bifurcation in the model, a rigorous analysis of this phenomenon using center manifold theory is proposed as a direction for future research. Additionally, incorporating fractional order derivatives could allow for a more accurate representation of memory effects, while the integration of stochastic differential equations could account for random fluctuations and parameter uncertainties, enhancing the robustness and predictive power of the model. It is important to note that the model was calibrated using gonorrhea infection data from the U.S. only, which may limit its applicability to regions with varying epidemiological profiles. Future studies should aim to incorporate more comprehensive datasets, including HPV prevalence, co-infection data, and information from diverse geographic and demographic contexts. These extensions would improve the applicability of the model and its value in informing targeted, evidence-based public health strategies.

CRediT authorship contribution statement

M. Arunkumar: Writing – review & editing, Writing – original draft, Visualization, Validation, Software, Resources, Methodology, Investigation, Formal analysis, Data curation, Conceptualization. **Sayooj Aby Jose:** Writing – review & editing, Validation, Supervision, Software, Project administration, Methodology, Investigation, Formal analysis, Data curation, Conceptualization. **K. Murugesan:** Writing – review & editing, Validation, Supervision, Investigation. **Anuwat Jirawattanapanit:** Writing – review & editing, Validation, Supervision, Project administration, Investigation, Funding acquisition.

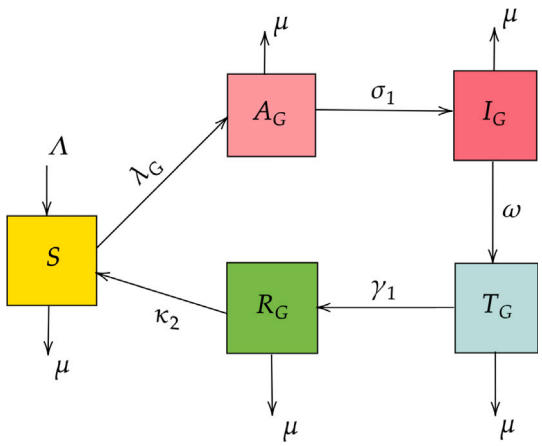

Fig. A.32. Schematic flow diagram of gonorrhea submodel.

Declaration of competing interest

The authors declare that they have no known competing financial interests or personal relationships that could have appeared to influence the work reported in this paper.

Acknowledgments

Dr. M. Arunkumar express his gratitude to the National Institute of Technology, Tiruchirappalli, India, for providing him an Institute Fellowship during his Ph.D program. He extends his sincere thanks to Mr. R. Azhagendran and Mr. M. Madhan Kumar for dedicating their valuable time and for their insightful discussions. Dr. Sayooj Aby Jose acknowledges the support received through the Global-LAMP Program of the National Research Foundation of Korea (NRF), funded by the Ministry of Education (Grant No. RS-2023-00301976). All authors express their gratitude to the Department of Mathematics, Faculty of Education, Phuket Rajabhat University, Thailand, for the invaluable support to the International Students Project Programme 2024. The authors also thank the Editor and the anonymous reviewers for their constructive comments, which have significantly improved the quality of this work.

Appendix A. Gonorrhea only submodel

By setting $V_H = A_H = I_H = R_H = I_{HG} = T_{HG}^G = 0$ in model (1), the deterministic system of nonlinear differential equations for gonorrhea submodel can be obtained as follows:

$$\begin{aligned}
\frac{dS}{dt} &= \Lambda - \lambda_G S - \mu S + \kappa_2 R_G,\\
\frac{dA_G}{dt} &= \lambda_G S - (\sigma_1 + \mu) A_G,\\
\frac{dI_G}{dt} &= \sigma_1 A_G - (\omega + \mu) I_G,\\
\frac{dT_G}{dt} &= \omega I_G - (\gamma_1 + \mu) T_G,\\
\frac{dR_G}{dt} &= \gamma_1 T_G - (\kappa_2 + \mu) R_G,
\end{aligned} \tag{A.1}$$

with nonnegative initial conditions

$$S(0) > 0, A_G(0) > 0, I_G(0) > 0, T_G(0) \geq 0, R_G(0) \geq 0. \tag{A.2}$$

Here $N = S + A_G + I_G + T_G + R_G$, and $\lambda_G = \dfrac{\beta_G(A_G + \phi_1 I_G + \phi_2 T_G)}{N}$. The schematic flow diagram that depicts the dynamics of the gonorrhea submodel is represented through Fig. A.32.

A.1. Biological well-posedness of the model (A.1)

Theorem A.1. *Any solution of the system (A.1), that is $(S(t), A_G(t), I_G(t), T_G(t), R_G(t))$ with initial conditions as in (A.2) remains nonnegative for all time $t \geq 0$. In other words, $\mathbb{R}^5_+$ is positively invariant with respect to system (A.1).*

Proof. The system (A.1) can be expressed as:

$$\dot{X}(t) = F(t, X),$$

where $X(t) = (S(t), A_G(t), I_G(t), T_G(t), R_G(t))^\top$, and $F(t, X) = (f_1(t, X), \ldots, f_5(t, X))^\top$ with the superscript $\top$ denoting the transpose. Following the tangent condition per hyperplane approach outlined in [58] (refer Property 1, Section 2.1.1), the proof examines the positive invariant of $\mathbb{R}^5_+$ by investigating the behavior of the vector field $(f_1, f_2, \ldots, f_5)^\top$ of (A.1) along its boundary hyperplane.

(i) **On $S = 0$ hyperplane:**
We note that $f_1 = \Lambda - \lambda_G S - \mu S + \kappa_2 R_G$ reduces to $f_1 = \Lambda + \kappa_2 R_G \geq 0$ on this hyperplane, implying that the vector field on this hyperplane is pointing to the interior of $\mathbb{R}^5_+$. Thus, no solutions can escape the interior of $\mathbb{R}^5_+$ through this hyperplane.

(ii) **On $A_G = 0$ hyperplane:**
We observe that $f_2 = \lambda_G S - (\sigma_1 + \mu)A_G$ becomes $f_2 = \dfrac{\beta_G(\phi_1 I_G + \phi_2 T_G)S}{S + I_G + T_G + R_G} \geq 0$, which implies $\dfrac{dA_G}{dt} \geq 0$ on this hyperplane. Using the same idea as in (i), it is observed that no solutions can escape the interior of $\mathbb{R}^5_+$ through this hyperplane.

(iii) **On remaining hyperplanes ($I_G = 0$, $T_G = 0$, and $R_G = 0$):** Similar computations confirm that $\dfrac{dI_G}{dt} \geq 0$, $\dfrac{dT_G}{dt} \geq 0$, and $\dfrac{dR_G}{dt} \geq 0$, respectively, on the corresponding boundary hyperplanes.

This analysis shows that solutions of system (A.1) with nonnegative initial conditions remain in the nonnegative region for all $t \geq 0$, thereby establishing that $\mathbb{R}^5_+$ is positively invariant with respect to system (A.1). □

Theorem A.2. *The solution of the system (A.1) is bounded in the biologically feasible region given by*

$$\Xi_1 = \left\{ (S, A_G, I_G, T_G, R_G) \in \mathbb{R}^5_+ : 0 \leq N \leq \frac{\Lambda}{\mu} \right\}.$$

Further, Ξ_1 is a positively invariant and attracting set.

Proof. Summing all the equations of the system (A.1) and solving gives

$$N(t) = N(0)\exp(-\mu t) + \frac{\Lambda}{\mu}(1 - \exp(-\mu t)), \tag{A.3}$$

where $N(0) = S(0) + A_G(0) + I_G(0) + T_G(0) + R_G(0)$. Now, if $N(0) \leq \dfrac{\Lambda}{\mu}$, then total population is bounded above by $\dfrac{\Lambda}{\mu}$. This ensures that the solution of the system (A.1) is bounded in the feasible region Ξ_1. Consequently, if the initial conditions of the system (A.1) start inside the region Ξ_1, then from (A.3), we ensure that the solution always remains within this region for all $t > 0$. This guarantees that Ξ_1 is a positively invariant set. The attractiveness of the region Ξ_1 follows directly from the more general argument presented in the proof of Theorem B.2. Therefore, the detailed proof is omitted here. □

The existence and uniqueness of solutions to system (A.1) follow from Theorem 3.3.

A.2. Existence of DFE and basic reproduction number

The disease-free equilibrium (DFE) point E°_G of the submodel (A.1) is computed to be

$$E^\circ_G = (S^\circ, A^\circ_G, I^\circ_G, T^\circ_G, R^\circ_G) = \left(\frac{\Lambda}{\mu}, 0, 0, 0, 0 \right).$$

The derivation of the basic reproduction number for the model (A.1), denoted by $\mathcal{R}_{0G}$, is carried out by employing the next generation matrix method [41]. Let $\overline{X}_G(t) = (A_G(t), I_G(t), T_G(t))^\top$. Accordingly, the system (A.1) can be represented as,

$$\frac{d\overline{X}_G}{dt} = \mathcal{F} - \mathcal{V},$$

where, $\mathcal{F}$ and $\mathcal{V}$ represent the new infection terms and the remaining transfer terms respectively, and are given by

$$\mathcal{F} = \begin{bmatrix} \lambda_G S \\ 0 \\ 0 \end{bmatrix} \text{ and } \mathcal{V} = \begin{bmatrix} (\mu + \sigma_1)A_G \\ -\sigma_1 A_G + (\mu + \omega)I_G \\ -\omega I_G + (\mu + \gamma_1)T_G \end{bmatrix}.$$

The next step involves computing the Jacobian matrices of $\mathcal{F}$ and $\mathcal{V}$ at E°_G.

$$F = \left.\frac{\partial \mathcal{F}}{\partial \overline{X}_G}\right|_{E^\circ_G} = \begin{bmatrix} \beta_G & \phi_1\beta_G & \phi_2\beta_G \\ 0 & 0 & 0 \\ 0 & 0 & 0 \end{bmatrix} \text{ and } V = \left.\frac{\partial \mathcal{V}}{\partial \overline{X}_G}\right|_{E^\circ_G} = \begin{bmatrix} \mu + \sigma_1 & 0 & 0 \\ -\sigma_1 & \mu + \omega & 0 \\ 0 & -\omega & \gamma_1 + \mu \end{bmatrix}.$$

The value of $\mathcal{R}_{0G}$ is determined by the largest eigenvalue (in magnitude) of the next generation matrix FV^{-1}. The eigenvalues of FV^{-1} are computed to be 0 (with algebraic multiplicity 2) and $\mathcal{R}_{0G}$, where

$$\mathcal{R}_{0G} = \frac{\beta_G((\omega + \mu)(\gamma_1 + \mu) + \phi_1\sigma_1(\gamma_1 + \mu) + \phi_2\sigma_1\omega)}{(\mu + \sigma_1)(\mu + \omega)(\gamma_1 + \mu)}.$$

Biologically, $\mathcal{R}_{0G}$ estimates the number of secondary gonorrhea infections caused by a single gonorrhea infected individual during their infectious phase.

A.3. Stability analysis

Theorem A.3. *The DFE point (E_G°) for the system (A.1) is locally asymptotically stable (LAS) if $\mathcal{R}_{0G} < 1$ and unstable if $\mathcal{R}_{0G} > 1$.*

Proof. The Jacobian matrix of the system (A.1) at E_G° is given by,

$$J^\circ = \begin{bmatrix} -\mu & -\beta_G & -\phi_1\beta_G & -\phi_2\beta_G & \kappa_2 \\ 0 & \beta_G - \mu - \sigma_1 & \phi_1\beta_G & \phi_2\beta_G & 0 \\ 0 & \sigma_1 & -\mu - \omega & 0 & 0 \\ 0 & 0 & \omega & -\gamma_1 - \mu & 0 \\ 0 & 0 & 0 & \gamma_1 & -\kappa_2 - \mu \end{bmatrix}.$$

The characteristic equation of the matrix J° can be derived from $|J^\circ - \xi I| = 0$, where I denotes the 5×5 identity matrix. The two eigenvalues of J° are computed as $\xi_1 = -\mu, \xi_2 = -\kappa_2 - \mu$, and the remaining three eigenvalues are the roots of the equation,

$$P(\xi) = \xi^3 + a_2\xi^2 + a_1\xi + a_0 = 0, \tag{A.4}$$

where, $a_0 = CDE - \beta_G DE - \phi_2\sigma_1\omega\beta_G - \phi_1\sigma_1\beta_G E, a_1 = CD + CE + DE - \beta_G D - \beta_G E - \phi_1\sigma_1\beta_G, a_2 = C + D + E - \beta_G$. Here, $C = \mu + \sigma_1$, $D = \mu + \omega$, and $E = \gamma_1 + \mu$.

For the system to be stable, all the eigenvalues of J° must have negative real parts. The negativity of ξ_1 and ξ_2 is evident, as all model parameters are assumed to be positive constants. Utilizing the Routh–Hurwitz criterion on Eq. (A.4), the remaining eigenvalues of J° can have negative real parts provided the following conditions are satisfied:

(i) $a_i > 0$, for $i = 0, 1, 2$, and
(ii) $a_2a_1 - a_0 > 0$.

Condition (i): Positivity of a_0, a_1, a_2:

Consider,

$$a_0 = CDE\left(1 - \frac{\beta_G(DE + \phi_2\sigma_1\omega + \phi_1\sigma_1 E)}{CDE}\right) = CDE(1 - \mathcal{R}_{0G}).$$

Thus, $a_0 > 0$ if $\mathcal{R}_{0G} < 1$.

Next, assuming $\mathcal{R}_{0G} < 1$, and using its definition from (4), we obtain the following relations:

(a) $1 > \mathcal{R}_{0G} > \dfrac{\beta_G}{C}$,
(b) $1 > \mathcal{R}_{0G} > \dfrac{\beta_G(DE + \phi_1\sigma_1 E)}{CDE} = \dfrac{\beta_G(D + \phi_1\sigma_1)}{CD}$.

These relations imply that if $\mathcal{R}_{0G} < 1$, then $C - \beta_G > 0$ and $CD - \beta_G(D + \phi_1\sigma_1) > 0$.

Now, a_1 can be written as $a_1 = \big(CD - \beta_G(D + \phi_1\sigma_1)\big) + (C - \beta_G)E + DE$.

Since all terms on the right-hand side are positive under the condition $\mathcal{R}_{0G} < 1$, it follows that $a_1 > 0$.

In addition, observe that $a_2 = (C - \beta_G) + D + E > 0$ if $\mathcal{R}_{0G} < 1$.

Condition (ii): Positivity of $a_2a_1 - a_0$:

$$a_2a_1 - a_0 = (C + E - \beta_G)a_1 + D\big(CD - \beta_G(D + \phi_1\sigma_1) + DE\big) + \phi_2\sigma_1\omega\beta_G + \phi_1\sigma_1\beta_G E.$$

Since each term in the above expression is positive when $\mathcal{R}_{0G} < 1$, it follows that $a_2a_1 - a_0 > 0$ under this condition. Therefore, the remaining three eigenvalues also have negative real parts only if $\mathcal{R}_{0G} < 1$.

Thus, the DFE point (E_G°) is LAS if $\mathcal{R}_{0G} < 1$ and unstable if $\mathcal{R}_{0G} > 1$. □

Next, we aim to verify whether the DFE point of the system (A.1) is globally asymptotically stable (GAS). To do this, let us state the following lemma from [59].

Lemma A.4. *If the system can be expressed as*

$$\frac{d\mathcal{X}}{dt} = \mathcal{P}(\mathcal{X}, \mathcal{K}),$$
$$\frac{d\mathcal{K}}{dt} = \mathcal{Q}(\mathcal{X}, \mathcal{K}) \text{ and } \mathcal{Q}(\mathcal{X}, \mathbf{0}) = \mathbf{0},$$

where $\mathcal{X} \in \mathbb{R}^m$ represents the uninfected compartments and $\mathcal{K} \in \mathbb{R}^n$ represents infected, asymptomatic and treated compartments, then the local asymptotic stability of the disease-free equilibrium $E^\circ = (\mathcal{X}^\circ, \mathbf{0})$ becomes global when the following conditions are satisfied:

(W1): $\mathcal{X}^\circ$ is GAS for the subsystem $\frac{d\mathcal{X}}{dt} = \mathcal{P}(\mathcal{X}, \mathbf{0})$.

(W2): If $\mathcal{Q}(\mathcal{X}, \mathcal{K}) = \mathcal{B}\mathcal{K} - \widehat{\mathcal{Q}}(\mathcal{X}, \mathcal{K})$, then $\widehat{\mathcal{Q}}(\mathcal{X}, \mathcal{K}) \geq \mathbf{0}$ for $(\mathcal{X}, \mathcal{K}) \in \Xi$, where Ξ is a biologically feasible region and $\mathcal{B} = D_{\mathcal{K}}\mathcal{Q}(\mathcal{X}^\circ, \mathbf{0})$ is a Metzler matrix.

Theorem A.5. *The DFE point (E_G°) for the system (A.1) is GAS if $\mathcal{R}_{0G} < 1$ and unstable if $\mathcal{R}_{0G} > 1$.*

Proof. Now for the system (A.1), let $\mathcal{X} = (S, R_G) \in \mathbb{R}^2$ and $\mathcal{K} = (A_G, I_G, T_G) \in \mathbb{R}^3$. To prove the condition $(W1)$, consider the reduced system of (A.1) as follows:

$$\begin{aligned} \frac{dS}{dt} &= \Lambda - \mu S + \kappa_2 R_G, \\ \frac{dR_G}{dt} &= -(\mu + \kappa_2) R_G. \end{aligned} \tag{A.5}$$

The solution of (A.5) is obtained as $S(t) = \frac{\Lambda}{\mu} - C_1 \exp(-(\mu + \kappa_2)t) + C_2 \exp(-\mu t)$ and $R_G(t) = C_1 \exp(-(\mu + \kappa_2)t)$. As $t \to \infty$, we obtain $S(t) \to \frac{\Lambda}{\mu}$ and $R_G(t) \to 0$. Thus the equilibrium point $\left(\frac{\Lambda}{\mu}, 0\right)$ is GAS for (A.5).

Next for the condition $(W2)$, consider

$$\mathcal{Q}(\mathcal{X}, \mathcal{K}) = \begin{bmatrix} \lambda_G S - (\sigma_1 + \mu) A_G \\ \sigma_1 A_G - (\omega + \mu) I_G \\ \omega I_G - (\gamma_1 + \mu) T_G \end{bmatrix},$$

and note that $\mathcal{Q}(\mathcal{X}, \mathbf{0}) = \mathbf{0}$. By computation, we get $\mathcal{B} = \begin{bmatrix} \beta_G - \mu - \sigma_1 & \phi_1 \beta_G & \phi_2 \beta_G \\ \sigma_1 & -\mu - \omega & 0 \\ 0 & \omega & -\gamma_1 - \mu \end{bmatrix}$.

Now, $\widehat{\mathcal{Q}}(\mathcal{X}, \mathcal{K})$ can be obtained as

$$\widehat{\mathcal{Q}}(\mathcal{X}, \mathcal{K}) = \begin{bmatrix} (1 - \frac{S}{N})(\beta_G(A_G + \phi_1 I_G + \phi_2 T_G)) \\ 0 \\ 0 \end{bmatrix}.$$

From the above, it is observed that $\widehat{\mathcal{Q}}(\mathcal{X}, \mathcal{K}) \geq \mathbf{0}$ for $(\mathcal{X}, \mathcal{K}) \in \Xi_1$. Using Lemma A.4, the DFE point E_G° of the system (A.1) is found to be GAS if $\mathcal{R}_{0G} < 1$. □

Appendix B. HPV only submodel

By setting $A_G = I_G = I_{HG} = T_G = T_{HG}^G = R_G = 0$ in model (1), the deterministic system of nonlinear differential equations for HPV submodel can be given by:

$$\begin{aligned} \frac{dS}{dt} &= (1 - \gamma)\Lambda - \lambda_H S + \theta V_H - (\vartheta + \mu) S + \kappa_1 R_H, \\ \frac{dV_H}{dt} &= \gamma \Lambda + \vartheta S - (1 - \epsilon)\lambda_H V_H - (\theta + \mu) V_H, \\ \frac{dA_H}{dt} &= \lambda_H S + (1 - \epsilon)\lambda_H V_H - (\sigma + \epsilon_1 + \mu + \delta_1) A_H, \\ \frac{dI_H}{dt} &= \sigma A_H - (\epsilon_2 + \mu + \delta_2) I_H, \\ \frac{dR_H}{dt} &= \epsilon_1 A_H + \epsilon_2 I_H - (\kappa_1 + \mu) R_H, \end{aligned} \tag{B.1}$$

with nonnegative initial conditions

$$S(0) > 0, V_H(0) \geq 0, A_H(0) > 0, I_H(0) > 0, R_H(0) \geq 0. \tag{B.2}$$

Here, $N = S + V_H + A_H + I_H + R_H$, and $\lambda_H = \frac{\beta_H(A_H + \psi_1 I_H)}{N}$. Fig. B.33 provides a visual representation of the HPV submodel.

B.1. Biological well-posedness of the model (B.1)

Theorem B.1. *Any solution of the system (B.1), that is $(S(t), V_H(t), A_H(t), I_H(t), R_H(t))$ with initial conditions as in (B.2) remains nonnegative for all time $t \geq 0$.*

Proof. The proof is based on similar arguments as outlined in the proof of Theorem A.1. □

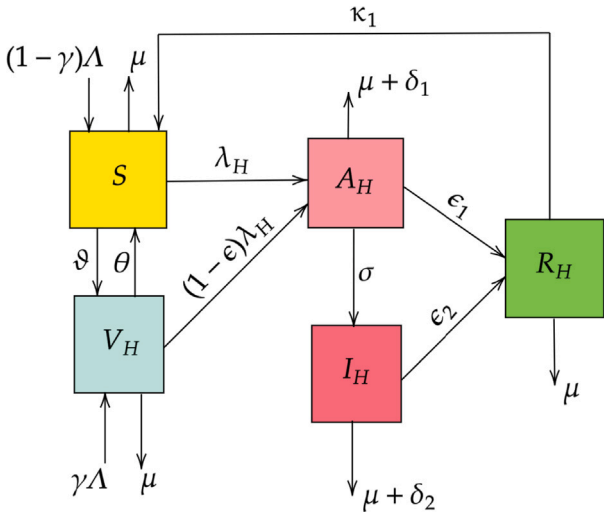

Fig. B.33. Flow diagram for HPV submodel.

Theorem B.2. *The solution of the system (B.1) is bounded in the biologically feasible region given by*

$$\Xi_2 = \left\{ (S, V_H, A_H, I_H, R_H) \in \mathbb{R}^5_+ : 0 \le N \le \frac{\Lambda}{\mu} \right\}.$$

Further, Ξ_2 is a positively invariant and attracting set.

Proof. Adding all the equations of the system (B.1) gives

$$\frac{dN}{dt} = \Lambda - \mu N - \delta_1 A_H - \delta_2 I_H \le \Lambda - \mu N. \tag{B.3}$$

According to Theorem 2.1.10 in [60], the solution to the above differential inequality is obtained as:

$$N(t) \le N(0)\exp(-\mu t) + \frac{\Lambda}{\mu}(1 - \exp(-\mu t)), \tag{B.4}$$

where $N(0) = S(0) + V_H(0) + A_H(0) + I_H(0) + R_H(0)$. Now, if $N(0) \le \frac{\Lambda}{\mu}$, then the arguments discussed in Theorem A.2 ensures that the solution of the system (B.1) is bounded in Ξ_2 and that Ξ_2 is positively invariant.

Next, let us prove the attractiveness of the region Ξ_2 by following the definition given in [38]. To do so, first let us show that there is some neighborhood U of Ξ_2 such that for all $x \in U$, the trajectory $\phi_t(x)$ satisfies $\phi_t(x) \in U$ for all $t \ge 0$.

Let $\delta > 0$. Consider the neighborhood U of Ξ_2 as $U = \left\{ (S, V_H, A_H, I_H, R_H) \in \mathbb{R}^5_+ : 0 \le N < \frac{\Lambda}{\mu} + \delta \right\}$. Let us take an initial value $x(0) = (S(0), V_H(0), A_H(0), I_H(0), R_H(0))$ in U. Now, consider the following two cases:

Case I: If $N(0) \le \frac{\Lambda}{\mu}$, then from (B.4), we obtain $N(t) \le \frac{\Lambda}{\mu}$ for all $t \ge 0$.

Case II: If $\frac{\Lambda}{\mu} < N(0) < \frac{\Lambda}{\mu} + \delta$, then from (B.3), $\left.\frac{dN}{dt}\right|_{t=0} < 0$, which implies $N(t)$ is decreasing on a neighborhood of 0. Also from (B.3), we obtain $\frac{dN}{dt} < 0$ whenever $N(t) > \frac{\Lambda}{\mu}$. This implies $N(t)$ is decreasing till it approaches the threshold value $\frac{\Lambda}{\mu}$.

Hence, in both cases, the trajectory $\phi_t(x)$ that starts in the region U will remain there itself.

Next, taking the limit superior as $t \to \infty$ in (B.4) yields $\limsup_{t\to\infty} N(t) \le \frac{\Lambda}{\mu}$. Let $\epsilon > 0$, then there exists $t^* > 0$ such that $N(t) < \limsup_{t\to\infty} N(t) + \epsilon$ for all $t \ge t^*$. That is, $N(t) - \frac{\Lambda}{\mu} < \epsilon$ for all $t \ge t^*$.

Now, let us prove $dist(\phi_t(x), \Xi_2) \to 0$ as $t \to \infty$, with respect to ℓ^1-norm. Let $t \ge t^*$. If $\phi_t(x) \in \Xi_2$, then $dist(\phi_t(x), \Xi_2) = 0$.

If $\phi_t(x) \notin \Xi_2$, then we can find $e = (S_e, V_{H_e}, A_{H_e}, I_{H_e}, R_{H_e}) \in \Xi_2$ such that $S_e + V_{H_e} + A_{H_e} + I_{H_e} + R_{H_e} = \Lambda/\mu$ and $\phi_t(x) \ge e$ (component-wise). Now,

$$\begin{aligned} dist(\phi_t(x), \Xi_2) &\leq \|\phi_t(x) - e\|_1, \\ &= |S(t) - S_e| + |V_H(t) - V_{H_e}| + |A_H(t) - A_{H_e}| + |I_H(t) - I_{H_e}| + |R_H(t) - R_{H_e}|, \\ &= S(t) + V_H(t) + A_H(t) + I_H(t) + R_H(t) - (S_e + V_{H_e} + A_{H_e} + I_{H_e} + R_{H_e}), \\ &< \frac{\Lambda}{\mu} + \epsilon - \frac{\Lambda}{\mu}, \\ &< \epsilon. \end{aligned}$$

Since $\epsilon > 0$ is arbitrary, we have $dist(\phi_t(x), \Xi_2) \to 0$ as $t \to \infty$. Hence, Ξ_2 is an attracting set. □

The existence and uniqueness of solutions to system (B.1) follow directly from Theorem 3.3.

B.2. Existence of DFE and basic reproduction number

The DFE point E_H° of the HPV subsystem (B.1) is computed as follows:

$$E_H^\circ = (S^\circ, V_H^\circ, A_H^\circ, I_H^\circ, R_H^\circ) = \left(\frac{\Lambda(\theta + (1-\gamma)\mu)}{\mu(\theta + \vartheta + \mu)}, \frac{\Lambda(\vartheta + \gamma\mu)}{\mu(\theta + \vartheta + \mu)}, 0, 0, 0 \right).$$

By utilizing the next generation matrix method as followed in Appendix A.2, the basic reproduction number for the HPV subsystem (B.1) is found to be $\mathcal{R}_{0H} = \frac{\beta_H(\theta + (1-\epsilon)\vartheta + (1-\gamma\epsilon)\mu)(\mu + \delta_2 + \epsilon_2 + \sigma\psi_1)}{(\theta + \mu + \vartheta)(\mu + \sigma + \epsilon_1 + \delta_1)(\mu + \delta_2 + \epsilon_2)}$. Here, $\mathcal{R}_{0H}$ estimates the average number of secondary HPV infections generated by one infected individual over the duration of their infectious period.

B.3. Stability analysis

Theorem B.3. *The DFE point (E_H°) for the system (B.1) is LAS if $\mathcal{R}_{0H} < 1$ and unstable if $\mathcal{R}_{0H} > 1$.*

Proof. Let J_1° denote the Jacobian matrix of the system (B.1) evaluated at E_H°. One of its eigenvalues is found to be $-(\kappa_1 + \mu)$. Two additional eigenvalues can be obtained from the polynomial

$$\xi^2 + ((\mu + \vartheta) + (\mu + \theta))\,\xi + \mu(\mu + \vartheta + \theta) = 0. \tag{B.5}$$

Since the coefficients of (B.5) are positive, the sum of its roots is negative and their product is positive. Hence both roots have negative real parts. The remaining two eigenvalues satisfy the polynomial

$$\xi^2 + (B + C - A)\xi + (BC - AC - \sigma\psi_1 A) = 0, \tag{B.6}$$

where, $A = \beta_H(1 - (\epsilon V_H^\circ/(S^\circ + V_H^\circ)))$, $B = \epsilon_1 + \mu + \sigma + \delta_1$, $C = \delta_2 + \epsilon_2 + \mu$. Through computation, the coefficients of (B.6) are found to be positive if $\mathcal{R}_{0H} < 1$. Therefore, by the Routh–Hurwitz criterion, the roots of (B.6) also possess negative real parts. Thus E_H° for the system (B.1) is LAS if $\mathcal{R}_{0H} < 1$ and unstable if $\mathcal{R}_{0H} > 1$. □

Theorem B.4. *The DFE point (E_H°) for the system (B.1) is GAS if $\mathcal{R}_{0H} < 1$ and unstable if $\mathcal{R}_{0H} > 1$.*

Proof. We utilize Lemma A.4 to prove this theorem. Now for the system (B.1), let $\mathcal{X} = (S, V_H, R_H) \in \mathbb{R}^3$ and $\mathcal{K} = (A_H, I_H) \in \mathbb{R}^2$. To prove the condition $(W1)$, consider the following subsystem

$$\begin{aligned} \frac{dS}{dt} &= (1-\gamma)\Lambda + \theta V_H - (\vartheta + \mu)S + \kappa_1 R_H, \\ \frac{dV_H}{dt} &= \gamma\Lambda + \vartheta S - (\theta + \mu)V_H, \\ \frac{dR_H}{dt} &= -(\kappa_1 + \mu)R_H. \end{aligned} \tag{B.7}$$

Solving (B.7) and then taking the limit as $t \to \infty$, it follows that $S(t) \to S^\circ, V_H(t) \to V_H^\circ, R_H(t) \to 0$. Thus $(S^\circ, V_H^\circ, 0)$ is GAS for the subsystem (B.7). Following the similar arguments as in Theorem A.5, the condition $(W2)$ in Lemma A.4 is also satisfied. Thus the DFE point E_H° of the system (B.1) is found to be GAS if $\mathcal{R}_{0H} < 1$. □

Appendix C. Proof of Theorem 3.4

The Jacobian matrix of the system (1) at E° is given by,

$$J_3^\circ = \begin{bmatrix} J_1^\circ & \mathcal{A}_{5\times 6} \\ O_{6\times 5} & J_2^\circ \end{bmatrix},$$

where J_1° denote the Jacobian matrix of the system (B.1) evaluated at E_H°, $O_{6\times5}$ is a zero matrix of order 6×5, $\mathcal{A}$ and J_2° are given below:

$$\mathcal{A}=\begin{bmatrix} \frac{-\mu S^\circ\beta_G}{\Lambda} & \frac{-\mu S^\circ\phi_1\beta_G}{\Lambda} & \frac{-\mu S^\circ(\phi_3\beta_G+\psi_2\beta_H)}{\Lambda} & \frac{-\mu\phi_2 S^\circ\beta_G}{\Lambda} & \frac{-\mu S^\circ(\beta_G\phi_4+\beta_H\psi_3)}{\Lambda} & \kappa_2\\ \frac{-\mu V_H^\circ\beta_G}{\Lambda} & \frac{-\mu V_H^\circ\phi_1\beta_G}{\Lambda} & \frac{-\mu V_H^\circ(\phi_3\beta_G+(1-\epsilon)\psi_2\beta_H)}{\Lambda} & \frac{-\mu V_H^\circ\phi_2\beta_G}{\Lambda} & \frac{-\mu V_H^\circ(\beta_G\phi_4+(1-\epsilon)\beta_H\psi_3)}{\Lambda} & 0\\ 0 & 0 & \frac{\mu\psi_2\beta_H(S^\circ+(1-\epsilon)V_H^\circ)}{\Lambda} & 0 & \frac{\mu\beta_H\psi_3(S^\circ+(1-\epsilon)V_H^\circ)}{\Lambda} & 0\\ 0 & 0 & 0 & \eta & 0 & 0\\ 0 & 0 & 0 & 0 & 0 & 0 \end{bmatrix},$$

$$J_2^\circ=\begin{bmatrix} \beta_G-\sigma_1-\mu & \phi_1\beta_G & \phi_3\beta_G & \phi_2\beta_G & \phi_4\beta_G & 0\\ \sigma_1 & -\mu-\omega & 0 & 0 & 0 & 0\\ 0 & 0 & -\delta_3-\mu-\omega_1 & 0 & 0 & 0\\ 0 & \omega & 0 & -\gamma_1-\mu & 0 & 0\\ 0 & 0 & \omega_1 & 0 & -\delta_4-\mu-\eta & 0\\ 0 & 0 & 0 & \gamma_1 & 0 & -\kappa_2-\mu \end{bmatrix}.$$

It follows from a property of block matrix that the eigenvalues of J_3° consist of the eigenvalues of both J_1° and J_2°. For the system (1) to be stable, all the eigenvalues of J_3° must have negative real parts. It is well known from Theorem B.3 that the eigenvalues of J_1° have negative real parts if $\mathcal{R}_{0H}<1$. Next our focus turns towards investigating the eigenvalues of J_2°. By expanding suitable columns, we can find three eigenvalues of J_2° such as $-\delta_3-\mu-\omega_1,-\delta_4-\mu-\eta,-\kappa_2-\mu$ and the remaining three eigenvalues are the roots of Eq. (A.4). From Theorem A.3, these eigenvalues have negative real parts if $\mathcal{R}_{0G}<1$. Thus for the co-infection model (1), E° is LAS if both $\mathcal{R}_{0G}<1$ and $\mathcal{R}_{0H}<1$. That is, the DFE point (E°) is LAS if $\mathcal{R}_0<1$ and unstable if $\mathcal{R}_0>1$.

Appendix D. Explicit expressions of constants used in boundary equilibrium

$$\begin{aligned}
C_1&=1+\psi_1\frac{\sigma}{\epsilon_2+\mu+\delta_2},\\
C_2&=\sigma+\epsilon_1+\mu+\delta_1,\\
C_3&=\frac{1}{\kappa_1+\mu}\left(\epsilon_1+\frac{\epsilon_2\sigma}{\epsilon_2+\mu+\delta_2}\right),\\
A_1&=(1-\gamma)\Lambda C_2(1-\epsilon)+\kappa_1C_3(1-\epsilon)\gamma\Lambda,\\
A_0&=(1-\gamma)\Lambda C_2(\theta+\mu)+\theta\gamma\Lambda C_2,\\
B_2&=(1-\epsilon)(C_2-\kappa_1C_3),\\
B_1&=C_2\big[(\theta+\mu)+(1-\epsilon)(\vartheta+\mu)\big]-\kappa_1C_3\big[(\theta+\mu)+(1-\epsilon)\vartheta\big],\\
B_0&=C_2\big[(\vartheta+\mu)(\theta+\mu)-\theta\vartheta\big],
\end{aligned}\qquad
\begin{aligned}
D_0&=\theta+\mu,\\
Q_2&=(1-\epsilon)(A_1+\gamma\Lambda B_2),\\
Q_1&=A_1D_0+A_0(1-\epsilon)+(1-\epsilon)(\gamma\Lambda B_1+\vartheta A_1),\\
Q_0&=A_0D_0+(1-\epsilon)(\gamma\Lambda B_0+\vartheta A_0),\\
K&=\delta_1+\frac{\delta_2\sigma}{\epsilon_2+\mu+\delta_2},\\
P_3&=(1-\epsilon)^2\Lambda C_2\big(K+\kappa_1C_3-C_2\big),\\
P_2&=KQ_1+\beta_HC_1\mu Q_2-C_2\Lambda(B_2D_0+B_1(1-\epsilon)),\\
P_1&=KQ_0+\beta_HC_1\mu Q_1-C_2\Lambda(B_1D_0+B_0(1-\epsilon)),\\
P_0&=\Lambda C_2^2\mu D_0(\vartheta+\mu+\theta)(\mathcal{R}_{0H}-1).
\end{aligned}$$

Appendix E. Analytical expressions for sensitivity of $\mathcal{R}_0$

As $\mathcal{R}_0=\max\{\mathcal{R}_{0G},\mathcal{R}_{0H}\}$, analytical expressions for the sensitivity of $\mathcal{R}_{0G}$ and $\mathcal{R}_{0H}$ with respect to model parameters are derived separately as follows:

$$\begin{aligned}
\Upsilon_{\beta_G}^{\mathcal{R}_{0G}}&=1,\\
\Upsilon_{\phi_1}^{\mathcal{R}_{0G}}&=\frac{\phi_1\sigma_1(\gamma_1+\mu)}{(\omega+\mu)(\gamma_1+\mu)+(\mu+\gamma_1)\phi_1\sigma_1+\phi_2\sigma_1\omega},\\
\Upsilon_{\phi_2}^{\mathcal{R}_{0G}}&=\frac{\phi_2\sigma_1\omega}{(\omega+\mu)(\gamma_1+\mu)+(\mu+\gamma_1)\phi_1\sigma_1+\phi_2\sigma_1\omega},\\
\Upsilon_{\omega}^{\mathcal{R}_{0G}}&=\frac{-\sigma_1\omega(\gamma_1\phi_1+\mu\phi_1-\mu\phi_2)}{(\mu+\omega)((\omega+\mu)(\gamma_1+\mu)+(\mu+\gamma_1)\phi_1\sigma_1+\phi_2\sigma_1\omega)},\\
\Upsilon_{\gamma_1}^{\mathcal{R}_{0G}}&=\frac{-\gamma_1\phi_2\sigma_1\omega}{(\gamma_1+\mu)((\omega+\mu)(\gamma_1+\mu)+(\mu+\gamma_1)\phi_1\sigma_1+\phi_2\sigma_1\omega)},\\
\Upsilon_{\sigma_1}^{\mathcal{R}_{0G}}&=\frac{\sigma_1((\gamma_1+\mu)(\mu\phi_1-(\mu+\omega))+\mu\phi_2\omega)}{(\mu+\sigma_1)((\omega+\mu)(\gamma_1+\mu)+(\mu+\gamma_1)\phi_1\sigma_1+\phi_2\sigma_1\omega)},\\
\Upsilon_{\beta_H}^{\mathcal{R}_{0H}}&=1,\\
\Upsilon_{\epsilon_1}^{\mathcal{R}_{0H}}&=\frac{-\epsilon_1}{\delta_1+\epsilon_1+\mu+\sigma},\\
\Upsilon_{\epsilon_2}^{\mathcal{R}_{0H}}&=\frac{-\epsilon_2\psi_1\sigma}{(\delta_2+\epsilon_2+\mu)(\delta_2+\epsilon_2+\mu+\psi_1\sigma)},
\end{aligned}\qquad
\begin{aligned}
\Upsilon_{\delta_1}^{\mathcal{R}_{0H}}&=\frac{-\delta_1}{\delta_1+\epsilon_1+\mu+\sigma},\\
\Upsilon_{\delta_2}^{\mathcal{R}_{0H}}&=\frac{-\delta_2\psi_1\sigma}{(\delta_2+\epsilon_2+\mu)(\delta_2+\epsilon_2+\mu+\psi_1\sigma)},\\
\Upsilon_{\epsilon}^{\mathcal{R}_{0H}}&=\frac{-\epsilon(\vartheta+\gamma\mu)}{\theta+\vartheta(1-\epsilon)+\mu(1-\epsilon\gamma)},\\
\Upsilon_{\vartheta}^{\mathcal{R}_{0H}}&=\frac{-\epsilon\vartheta(\theta+(1-\gamma)\mu)}{(\mu+\theta+\vartheta)(\theta+\vartheta(1-\epsilon)+\mu(1-\epsilon\gamma))},\\
\Upsilon_{\gamma}^{\mathcal{R}_{0H}}&=\frac{-\epsilon\gamma\mu}{\theta+\vartheta(1-\epsilon)+\mu(1-\epsilon\gamma)},\\
\Upsilon_{\sigma}^{\mathcal{R}_{0H}}&=\frac{-\sigma(\delta_2+\epsilon_2+\mu-\psi_1(\delta_1+\epsilon_1+\mu))}{(\delta_1+\epsilon_1+\mu+\sigma)(\delta_2+\epsilon_2+\mu+\psi_1\sigma)},\\
\Upsilon_{\theta}^{\mathcal{R}_{0H}}&=\frac{\epsilon\theta(\vartheta+\gamma\mu)}{(\mu+\theta+\vartheta)(\theta+\vartheta(1-\epsilon)+\mu(1-\epsilon\gamma))},\\
\Upsilon_{\psi_1}^{\mathcal{R}_{0H}}&=\frac{\psi_1\sigma}{\delta_2+\epsilon_2+\mu+\psi_1\sigma}.
\end{aligned}$$

References

[1] World Health Organization, Sexually Transmitted Infections (STIs) – Fact sheet, 2024, (Accessed 03 August 2024).URL https://www.who.int/news-room/fact-sheets/detail/sexually-transmitted-infections-(stis).

[2] World Health Organization, Human papillomavirus and cancer – fact sheet, 2024, (Accessed 03 August 2024). URL https://www.who.int/news-room/fact-sheets/detail/human-papilloma-virus-and-cancer.

[3] E. Meites, Human papillomavirus vaccination for adults: updated recommendations of the advisory committee on immunization practices, MMWR Morb. Mortal. Wkly. Rep. 68 (2019) http://dx.doi.org/10.15585/mmwr.mm6832a3.

[4] Centers for Disease Control and Prevention, Human papillomavirus (HPV), 2024, (Accessed 03 August 2024). URL https://www.cdc.gov/hpv/about/index.html.

[5] Centers for Disease Control and Prevention, Gonorrhea – CDC detailed fact sheet, 2024, (Accessed 03 August 2024). URL https://www.cdc.gov/std/gonorrhea/stdfact-gonorrhea-detailed.htm.

[6] World Health Organization, Gonorrhoea (*Neisseria gonorrhoeae* infection), 2024, (Accessed 03 August 2024). URL https://www.who.int/news-room/fact-sheets/detail/gonorrhoea-(neisseria-gonorrhoeae-infection).

[7] S. Muthukumar, K. Myilsamy, A. Balakumar, V. Chinnadurai, Nonlinear analysis and dynamics of COVID-19 mathematical model with optimal control strategies, Optim. Control. Appl. Methods 44 (5) (2023) 2838–2860, http://dx.doi.org/10.1002/oca.3006.

[8] M. Arunkumar, P.K. Rajan, K. Murugesan, Mathematical analysis of an optimal control problem for mitigating HPV transmission and cervical cancer progression through educational campaigns, Iran. J. Sci. 49 (5) (2025) 1309–1325, http://dx.doi.org/10.1007/s40995-025-01804-2.

[9] S.A. Jose, C. Jisha, O. Boubaker, Mathematical and AI-based approaches in epidemiology: Foundations and frontiers, in: Mathematical Modeling and AI-Driven Computational Techniques for Epidemiology and Disease Dynamics, Elsevier, 2026, pp. 3–27.

[10] E.H. Elbasha, Global stability of equilibria in a two-sex HPV vaccination model, Bull. Math. Biol. 70 (2008) 894–909, http://dx.doi.org/10.1007/s11538-007-9283-0.

[11] O. Sharomi, T. Malik, A model to assess the effect of vaccine compliance on human papillomavirus infection and cervical cancer, Appl. Math. Model. 47 (2017) 528–550, http://dx.doi.org/10.1016/j.apm.2017.03.025.

[12] M. Al-arydah, R. Smith, An age-structured model of human papillomavirus vaccination, Math. Comput. Simulation 82 (4) (2011) 629–652, http://dx.doi.org/10.1016/j.matcom.2011.10.006.

[13] K. Zhang, X.W. Wang, H. Liu, Y.P. Ji, Q. Pan, Y.M. Wei, X. Ma, Mathematical analysis of a human papillomavirus transmission model with vaccination and screening, Math. Biosci. Eng. 17 (5) (2020) 5449–5476, http://dx.doi.org/10.3934/mbe.2020294.

[14] F. Saldaña, J.A. Camacho-Gutiérrez, G. Villavicencio-Pulido, J.X. Velasco-Hernandez, Modeling the transmission dynamics and vaccination strategies for human papillomavirus infection: An optimal control approach, Appl. Math. Model. 112 (2022) 767–785, http://dx.doi.org/10.1016/j.apm.2022.08.017.

[15] S. Gao, M. Martcheva, H. Miao, L. Rong, A two-sex model of human papillomavirus infection: Vaccination strategies and a case study, J. Theoret. Biol. 536 (2022) 111006, http://dx.doi.org/10.1016/j.jtbi.2022.111006.

[16] K.L. Cooke, J.A. Yorke, Some equations modelling growth processes and gonorrhea epidemics, Math. Biosci. 16 (1–2) (1973) 75–101, http://dx.doi.org/10.1016/0025-5564(73)90046-1.

[17] A. Lajmanovich, J.A. Yorke, A deterministic model for gonorrhea in a nonhomogeneous population, Math. Biosci. 28 (3–4) (1976) 221–236, http://dx.doi.org/10.1016/0025-5564(76)90125-5.

[18] S. Mushayabasa, C. Bhunu, Modelling the effects of heavy alcohol consumption on the transmission dynamics of gonorrhea, Nonlinear Dynam. 66 (2011) 695–706, http://dx.doi.org/10.1007/s11071-011-9942-4.

[19] A. Gkana, L. Zachilas, Bifurcations and chaos in discrete-time gonorrhea model, Chaotic Model. Simul. 1 (2015) 51–64.

[20] I.I. Adamu, S. Usman, Mathematical model for the dynamics of neisseria gonorrhea disease with natural immunity and treatment effects, J. Math. Res. 10 (2) (2018) http://dx.doi.org/10.5539/jmr.v10n2p151.

[21] About cervical cancer - risk factors, 2024, (Accessed 03 August 2024). URL https://www.cancer.columbia.edu/cancer-types-care/types/cervical-cancer/about-cervical-cancer.

[22] Z. Lu, P. Zhao, H. Lu, M. Xiao, Analyses of human papillomavirus, *Chlamydia trachomatis, Ureaplasma urealyticum, Neisseria gonorrhoeae*, and co-infections in a gynecology outpatient clinic in haikou area, China, BMC Women's Health 23 (1) (2023) 117, http://dx.doi.org/10.1186/s12905-023-02259-6.

[23] N.L. Kops, M. Bessel, J.D.C. Horvath, C. Domingues, F.M.A. de Souza, A.S. Benzaken, G.F.M. Pereira, A.G.K. Maranhão, L.L. Villa, B. Mello, E.M. Wendland, Factors associated with HPV and other self-reported STI coinfections among sexually active Brazilian young adults: cross-sectional nationwide study, BMJ Open 9 (6) (2019) e027438, http://dx.doi.org/10.1136/bmjopen-2018-027438.

[24] E. Bukowska, B. Młynarczyk-Bonikowska, M. Malejczyk, G. Przedpełska, S.W. de Walthoffen, G. Młynarczyk, S. Majewski, Human papillomavirus (HPV) coinfection with other sexually transmitted infections in patients of the Department of Dermatology and Venereology at the Medical University of Warsaw, Dermatol. Review/Przeglkad Dermatol. 107 (2) (2020) 138–147, http://dx.doi.org/10.5114/dr.2020.96355.

[25] S. Lenhart, J.T. Workman, Optimal Control Applied To Biological Models, Chapman & Hall/CRC, 2007.

[26] M. Arunkumar, Unraveling the dynamics of trichomoniasis transmission: Modeling reinfection and asymptomatic spread with optimal control strategies based on united states demographics, Phys. Scr. (2026) http://dx.doi.org/10.1088/1402-4896/ae3ccd.

[27] N. Ringa, M. Diagne, H. Rwezaura, A. Omame, S. Tchoumi, J. Tchuenche, HIV and COVID-19 co-infection: A mathematical model and optimal control, Informatics Med. Unlocked 31 (2022) 100978, http://dx.doi.org/10.1016/j.imu.2022.100978.

[28] C.M. Pinto, A.R. Carvalho, New findings on the dynamics of HIV and TB coinfection models, Appl. Math. Comput. 242 (2014) 36–46, http://dx.doi.org/10.1016/j.amc.2014.05.061.

[29] E.C. Chukukere, A. Omame, C. Onyenegecha, S. Inyama, Mathematical analysis of a model for chlamydia and gonorrhea codynamics with optimal control, Results Phys. 27 (2021) 104566, http://dx.doi.org/10.1016/j.rinp.2021.104566.

[30] A. Omame, C. Nnanna, S. Inyama, Optimal control and cost-effectiveness analysis of an HPV–chlamydia trachomatis co-infection model, Acta Biotheor. 69 (2021) 185–223, http://dx.doi.org/10.1007/s10441-020-09401-z.

[31] A. Omame, D. Okuonghae, U. Nwafor, B. Odionyenma, A co-infection model for HPV and syphilis with optimal control and cost-effectiveness analysis, Int. J. Biomath. 14 (07) (2021) 2150050, http://dx.doi.org/10.1142/S1793524521500509.

[32] M. Arunkumar, K. Murugesan, Modeling optimal control strategies for HIV and gonorrhea co-infection: Incorporating screening along with treatment, Phys. Scr. 99 (12) (2024) 125037, http://dx.doi.org/10.1088/1402-4896/ad8afc.

[33] M.A. Hye, M.H.A. Biswas, M.F. Uddin, M. Saifuddin, Mathematical modeling of COVID-19 and dengue co-infection dynamics in Bangladesh: optimal control and data-driven analysis, Comput. Math. Model. 33 (2) (2022) 173–192, http://dx.doi.org/10.1007/s10598-023-09580-7.

[34] P.M. Mwamtobe, S.M. Simelane, S. Abelman, J.M. Tchuenche, Optimal control of intervention strategies in malaria–tuberculosis co-infection with relapse, Int. J. Biomath. 11 (02) (2018) 1850017, http://dx.doi.org/10.1142/S1793524518500171.

[35] M.M. Ojo, T.O. Benson, O.J. Peter, E.F.D. Goufo, Nonlinear optimal control strategies for a mathematical model of COVID-19 and influenza co-infection, Phys. A 607 (2022) 128173, http://dx.doi.org/10.1016/j.physa.2022.128173.

[36] A. Omame, M. Abbas, Modeling SARS-CoV-2 and HBV co-dynamics with optimal control, Phys. A 615 (2023) 128607, http://dx.doi.org/10.1016/j.physa.2023.128607.

[37] H. Rwezaura, M. Diagne, A. Omame, A. de Espindola, J. Tchuenche, Mathematical modeling and optimal control of SARS-CoV-2 and tuberculosis co-infection: a case study of Indonesia, Model. Earth Syst. Environ. 8 (4) (2022) 5493–5520, http://dx.doi.org/10.1007/s40808-022-01430-6.
[38] L. Perko, Differential Equations and Dynamical Systems, vol. 7, Springer Science & Business Media, 2013, http://dx.doi.org/10.1007/978-1-4613-0003-8.
[39] H.R. Thieme, Mathematics in Population Biology, Princeton University Press, 2018.
[40] O. Diekmann, J.A.P. Heesterbeek, J.A. Metz, On the definition and the computation of the basic reproduction ratio $\mathcal{R}_0$ in models for infectious diseases in heterogeneous populations, J. Math. Biol. 28 (1990) 365–382, http://dx.doi.org/10.1007/BF00178324.
[41] P. van den Driessche, J. Watmough, Reproduction numbers and sub-threshold endemic equilibria for compartmental models of disease transmission, Math. Biosci. 180 (2002) 29–48, http://dx.doi.org/10.1016/S0025-5564(02)00108-6.
[42] Census, Age and sex composition in the United States, 2012, (Accessed 03 August 2024). URL https://www.census.gov/data/tables/2012/demo/age-and-sex/2012-age-sex-composition.html.
[43] Centers for Disease Control and Prevention, Life expectancy (years) in United States of America, 2024, (Accessed 03 August 2024). URL https://datacommons.org/place/country/USA.
[44] Centers for Disease Control and Prevention, Sexually transmitted disease surveillance 2012, Atlanta: U. s. Department of health and human services, 2013, (Accessed 03 August 2024). URL http://www.cdc.gov/std/stats.
[45] National Cancer Institute, Accelerating HPV vaccine uptake: Urgency for action to prevent cancer. a report to the president of the United States from the president's cancer panel. Bethesda, MD: National cancer institute, 2014, (Accessed 03 August 2024)URL http://deainfo.nci.nih.gov/advisory/pcp/annualReports/HPV/index.htm.
[46] Centers for Disease Control and Prevention, About HPV vaccines, 2024, (Accessed 03 August 2024). URL https://www.cdc.gov/vaccines/vpd/hpv/hcp/vaccines.html.
[47] National Cancer Institute, Cancer trends progress report, NIH, DHHS, Bethesda, MD, 2024, (Accessed 03 August 2024)URL https://progressreport.cancer.gov.
[48] Centres for Disease Control and Prevention, Sexually transmitted infections surveillance, 2022, (Accessed 03 August 2024). URL https://www.cdc.gov/std/statistics/2022/default.htm.
[49] A. Omame, R. Umana, D. Okuonghae, S. Inyama, Mathematical analysis of a two-sex human papillomavirus (HPV) model, Int. J. Biomath. 11 (07) (2018) 1850092, http://dx.doi.org/10.1142/S1793524518500924.
[50] Centers for Disease Control and Prevention, About genital HPV infection, 2024, (Accessed 03 August 2024). URL https://www.cdc.gov/sti/about/about-genital-hpv-infection.html.
[51] A. Omame, D. Okuonghae, R. Umana, S. Inyama, Analysis of a co-infection model for HPV-TB, Appl. Math. Model. 77 (2020) 881–901, http://dx.doi.org/10.1016/j.apm.2019.08.012.
[52] T. Malik, J. Reimer, A. Gumel, E.H. Elbasha, S. Mahmud, The impact of an imperfect vaccine and pap cytology screening on the transmission of human papillomavirus and occurrence of associated cervical dysplasia and cancer, Math. Biosci. Eng. 10 (4) (2013) 1173–1205, http://dx.doi.org/10.3934/mbe.2013.10.1173.
[53] N. Chitnis, J.M. Hyman, J.M. Cushing, Determining important parameters in the spread of malaria through the sensitivity analysis of a mathematical model, Bull. Math. Biol. 70 (2008) 1272–1296, http://dx.doi.org/10.1007/s11538-008-9299-0.
[54] W.H. Fleming, R.W. Rishel, Deterministic and stochastic optimal control, vol. 1, Springer Science & Business Media, 2012.
[55] T.T. Yusuf, A. Abidemi, Effective strategies towards eradicating the tuberculosis epidemic: An optimal control theory alternative, Heal. Anal. 3 (2023) 100131, http://dx.doi.org/10.1016/j.health.2022.100131.
[56] T.T. Yusuf, F. Benyah, Optimal strategy for controlling the spread of HIV/AIDS disease: a case study of South Africa, J. Biol. Dyn. 6 (2) (2012) 475–494, http://dx.doi.org/10.1080/17513758.2011.628700.
[57] L.S. Pontryagin, Mathematical Theory of Optimal Processes, CRC Press, 1987.
[58] M.Y. Li, An Introduction to Mathematical Modeling of Infectious Diseases, vol. 2, Springer, 2018.
[59] C. Castillo, Z. Feng, W. Huang, On the computation of $\mathcal{R}_0$ and its role on global stability, in: Mathematical approaches for emerging and reemerging infectious diseases: An introduction, 2002, pp. 229–250.
[60] A. Stuart, A.R. Humphries, Dynamical Systems and Numerical Analysis, vol. 2, Cambridge University Press, 1998.